Parametric Exploration of Shading Screens:
Daylight, Sun Penetration, and view Factor

Doaa Alsharif

A Thesis
submitted in partial fulfillment of the
requirements for the degree of

Master of Science in Architecture

University of Washington

2017

Committee:
Mehlika Inanici
Chris Meek

Program Authorized to Offer Degree:

Architecture

University of Washington

Abstract

Parametric Exploration of Shading Screens:
Daylight, Sun Penetration, and view Factor

Doaa Alsharif

Chair of the Supervisory Committee:
Associate Professor Mehlika Inanici
Architecture

Parametric Exploration of Shading Screens investigates a suite of performance criteria that can be used to select a shading screen. Shading screens can be effective means of controlling sun penetration and daylight availability in a given space. The evaluation criteria varies depending on the functionality of the space and the intended visual effect. It is possible to achieve diffuse or dynamic environments, bright or dim spaces, with the right light levels and the control of glare. A combination of a variety of screen patterns and openness factors are created using parametric modeling techniques and evaluated using daylighting simulations. The outcome is a workflow to create and select the right shading screen to design the luminous environment for the intended visual effect, visual comfort, and performance.

Table of Contents

LIST OF FIGURES

LIST OF FIGURES

LIST OF FIGURES

CHAPTER 1
INTRODUCTION

Screens (Figure1) act as a design element for transparent facades and play a vital role in the performance of a building, especially to prevent excessive heat gain and to provide visual comfort. This study looks at the science behind the design and analysis of shading screens inspired by Islamic geometries and ornamental patterns. These screens are extensively used in hot arid and hot humid climates in the Middle East, Turkey, Iran, India and Spain. They are known to be very effective in providing sun control and maximizing diffuse lighting. In recent years, complex and dynamic sun screens are being more frequently used in modern buildings (Figure 2).
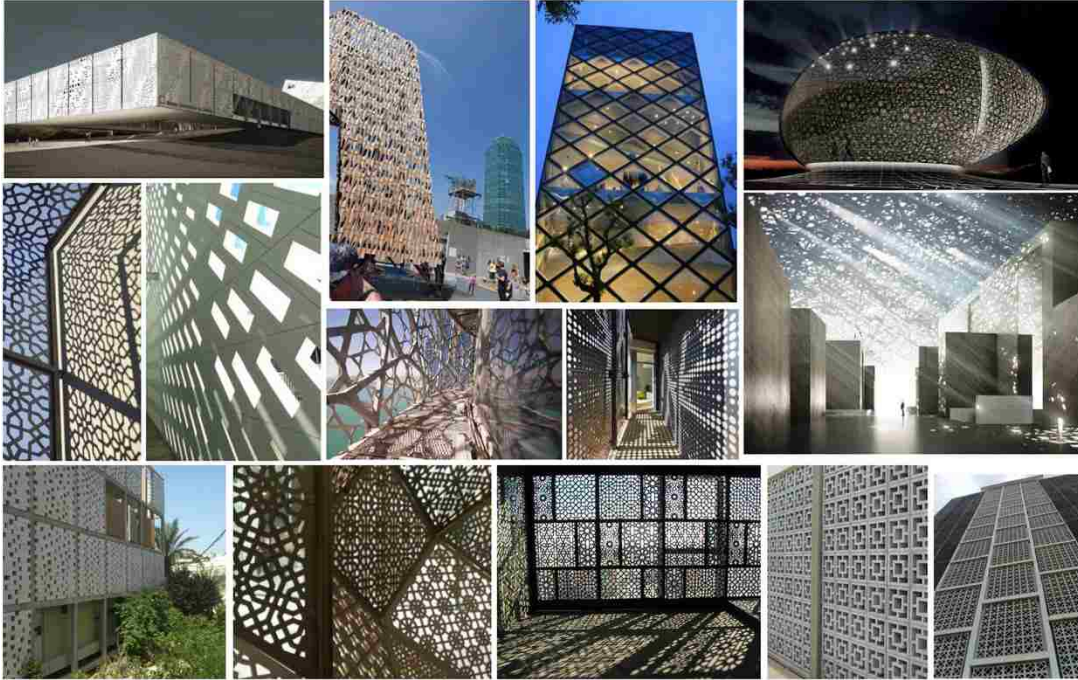
Figure 1: Various shapes and sizes of different facades around the world: The CHN Arquitos, Exploratory Science Museum of Unicamp Sao Paulo, Brazil, The Elsye Alam Architects Alam Family house in Jakarta, Indonesia, The Doha Tower in Abu Dhabi, The Louver in AbuDhabi.

Figure 2: Modern use of screens: Braod Museum LA, Art museum, Aspen, Nike, Scottsdale.

6

The earliest evidence on use of perforated screens "Mashrabiyas or wooden screens" goes back to the twelfth century in Bagdad during the Abbasid period (from 750 – 1261) (Holl, 2011). The crafts tradition that produces Islamic geometric designs is based on methods requiring geometrical and mathematical skills. Artisans and master builders used traditional tools like the compass and a ruler to create geometrical patterns.

Explaining unfamiliar terms:

"Roshan" is an Arabic word that has a Persian root which means "Aperture". It behaves like a bay window, where people can sit and lookout. Similar to "Mashrabiya" and some call it "Mashrafiya". "Mashrabiya" means the clay jug or pot where water is kept, and that's because it is known to place these clay jugs around the Masharbiya to get cool. "Mashrafiya" on the other hand, is a compound word meaning "Look and Drink". Roshans and Mashrabiyas can be found in the Middle east, north Africa, Spain, Iran and Turkey. Jaalis on the other hand, are found in India. Jaali in Hindi means "net". They differ from Roshan and Mashrabiyas in their patterns, they can be made with plant and floral patterns unlike the others which are made from geometrical patterns. However, all of them serve the same purpose, to protect from sun and severe climate conditions, cool water and provide privacy "see without being seen" (Figure3) (Hillenbrand, 2004).

Roshan   Jaali   Mashrabiya
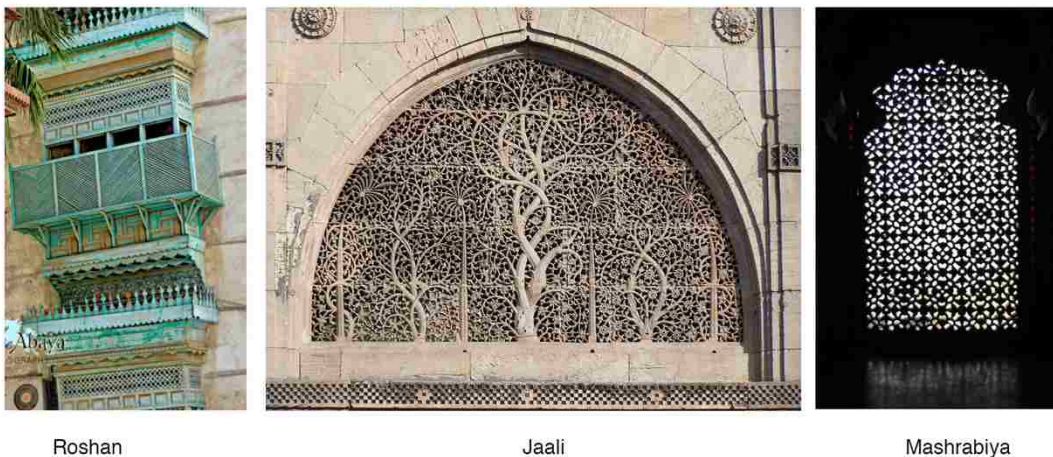
Figure 3: Explain unfamiliar terms.

Artist John Fredrick Lewis among others, drew many pictures (Figure4) of the Mashrabiya with women behind it as an example of how these were used for privacy. In the Islamic culture, women are not allowed to be seen, so the mashrabiya serves them to see others without wearing their vail.

Figure 4: "The reception" 1973, Artist: John Fredrick Lewis

In 2013, architect Sandeep Khosla won the education category at Inside Festival in Singapore for his design (Hobson, 2013). He used the Mashrabiya with two different floral patterns in a kindergarten school called "DPS" in India. He used it as a tool in creating natural ventilation to keep the classrooms cool without the use of AC (Figure 5).

Figure 5: Floral patterns, DPS Kindergarten school in India.

In the last few years, there has been a growing interest in designing and fabricating these patterns. Parametric modeling tools enable us to create complex and dynamic sun screens, and fabrication tools allow us to manufacture them. The demand to create and fabricate shade fabrics has driven the market to create solutions. For instance, Zahner, an Architecture company developed a platform (Figure 6) for clients to design their own screens and provide instant pricing. Once the client is satisfied with their creation, they could upload them for fabrication.
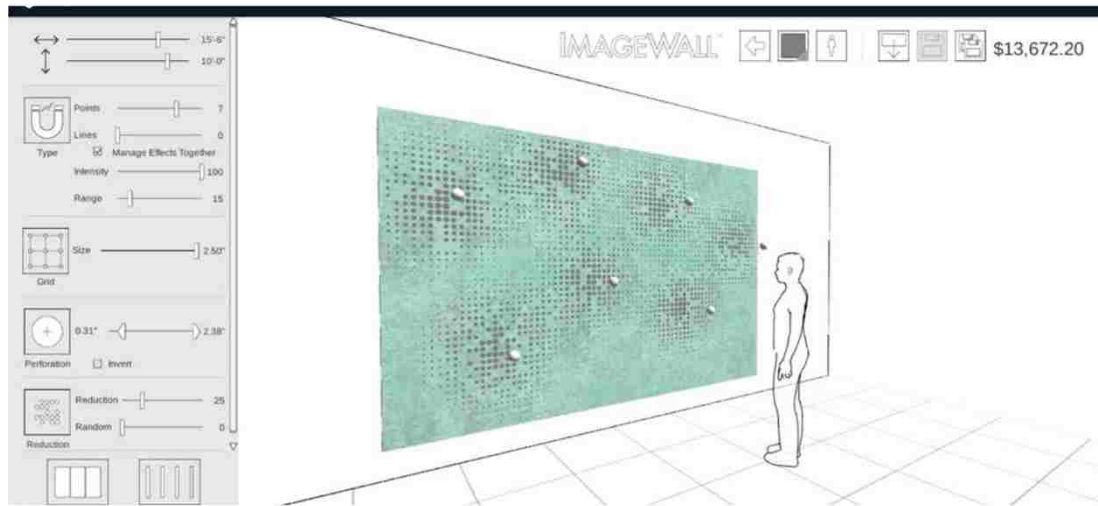
Figure 6: ShopFLoor, Zahner Tool for fabricating screens.

The tool created by Zahner enables almost infinite ways of creating sun screens, but the main questions that emerge from the availability of the tool is that "how are clients choosing their designs?", "how would it perform?", "which openness factor should they choose?", "how big or how thick should their screens be?". There is no straightforward answer, as it would depend on many factors such as the site, the climate, the building design, the functionality of the space, design concept; and the list goes on. There is a need to develop a workflow to answer these questions, and this thesis addresses to this gap. The objective is to use example patterns to reflect on the methodologies for pattern generation and pattern evaluation. Factors that have impact on performance are identified and parametrized; evaluation techniques that are meaningful for selecting a particular pattern have been distilled from a potential of candidate metrics; and selection criteria has been applied to a variety of spaces that range from controlled work environments to playful luminous environments.

The thesis is organized as follows: Chapter 2 provides a literature review of currently available techniques for designing shading devices. Chapter 3 investigates techniques and workflows to creating patterns that overcomes computational and simulation challenges . Chapter 4 presents the results based on the simulations and scenarios where these result could be used. Chapter 4 concludes and summarize the findings of this thesis.

CHAPTER 2
DESIGNING SHADING DEVICES

High performance facades are building envelopes that integrate and regulate external environmental factors to create energy efficient, healthy, productive and comfortable indoor environments for the occupants. Although "high performance buildings" is a relatively new terminology and U.S. Department of Energy has been maintaining a database of High Performance Buildings since 2012 (DOE, 2016), the wisdom of creating efficient and comfortable environments have a long history. "Design with climate", "climate conscious building design", "bioclimatic architecture", green buildings, and "sustainable design" are some of the terminology (Olgyay and Olgyay 1963; Schiller and Evans1994; Mumovic and Santamouris 2009; 7 group and Reeds, 2009) that precedes the use of "high performance buildings". Successful examples are particularly prevalent in vernacular architecture. These buildings adapt to the climatic regions they are located by responding to environmental factors such as solar radiation, daylight availability, humidity, and airflow.

Different climatic regions pose different set of design challenges and opportunities. For example, cold climates benefit from compact building forms that utilize strategies for maximizing the passive solar heating, and adequate insulation for minimizing the heat loss. The igloo (Figure7) is a well-known solution for this condition. It is designed to orient the entrance away from prevailing wind and prevent warm air to escape. The interior temperature can reach 15⬚C (60⬚F) while it's -26⬚C (-15⬚F) on the outside. Canada, with a less extreme climate, homes are joined together with double shells -that are removable in summer months for ventilation- to reduce surface exposure. In hot arid climates, compact building forms are preferred to provide self-shading; and external shading devices are employed to block sun rays. Opaque materials that have heat storing capacities, like stone and brick, are used to protect the building from unwanted heat gain or loss. Pueblo, in San Juan was constructed with adobe roofs and walls which have a high insulation value and windows were small to prevent the glary sun (Figure 8). Hot humid climates face two problems, excessive heat and moisture. This type of climate favors building types that are individual and elevated that encourages air movements. Gable roofs with steep angle and overhang covered with grass insulate and shade the building. (Figure 9). Temperate climates permit flexibility in design, where a balance between solar exposure, solar control, and daylight availability is achieved by shading the building during the cooling season and collecting solar energy during the heating seasons (Olgyay and Olgyay 1963).

Figure 7: Igloo-Cold Dry Climate

Figure 8: Pueblo - Hot arid Climate

Figure 9: Hot humid Climate

Utilization of daylight in all climates is provided by effectively sizing the daylight apertures and employing control strategies such as static and movable shading devices and light shelves to provide adequate levels of light throughout the daily and seasonal variations of sun position and cloud cover. The aesthetics of these buildings derive inspiration from their environments and the material choices are based on readily available local materials. What makes these buildings sustainable is that they allow adequate amounts of daylight, solar energy, air and moisture into the interiors when it is needed, and prevent it when it is unwanted. The patterns of control and utilization of environmental factors is highly climate dependent, and they are designed with considerations that include building geometry, materials, orientation, building type, occupancy patterns, and equipment loads (Lee et al., 2002).

In the last 30 years, new computational methods have been developed to facilitate the design process. These tools have introduced many capabilities and challenges in the design process. They help the designer to push the boundaries of acceptable design solutions and explore the complexity of the built environment through new toolsets. The driving idea behind using robust simulations and analysis techniques in design process is to study the individual and unique criteria for each building, program, and site that cannot be addressed simply by generic rules of thumb or guidelines. The challenges in the effective use of these tools include their inherent learning curves, and how well they adapt to problem solving for specific problems, and how well they can be integrated into the performance oriented design processes.

In order to understand the process of designing high performance buildings, it is important to study the main source of light: the sun, it's position, and movement in the sky. The sun is 93 miles away from earth and the solar radiation reaching the earth's atmosphere remains relatively constant throughout the year at 1367 W/m2 (433 Btu/ft2). However, the length of the atmosphere the sun rays travel, the cloud cover, and atmospheric turbidity has a significant impact on the amount of direct and diffuse solar radiation reaching to earth's surface (Stein et al., 2006). The orientation and the slope of a surface, the neighboring structures that block and/or reflect solar rays will further impact the amount of radiation received on a given surface.

A clear understanding of the movement of the sun and the local climatic conditions enables designers to design high performing facades. Shading systems provide the single most effective strategy for façade designs to achieve visual and thermal occupant comfort along with building energy efficiency. There are few different approaches to shading devices. They are grouped here based on their design criteria; but the categorization also reflects on the chronological development and the advancement of the shading system design and evaluation techniques.
 a. Shading designs based on solar geometry;
 b. Shading designs based on available solar radiation (insolation);
 c. Shading devices based on space heating and cooling loads; and
 d. Shading devices based on occupant visual comfort.

The following 4 subsections discuss these 4 strategies. For each strategy, the design technique is described; and currently available computational tools are utilized to illustrate each

1- Solar Geometry 2- Incident Solar Radiation 3- Energy Loads 4- Visual Comfort
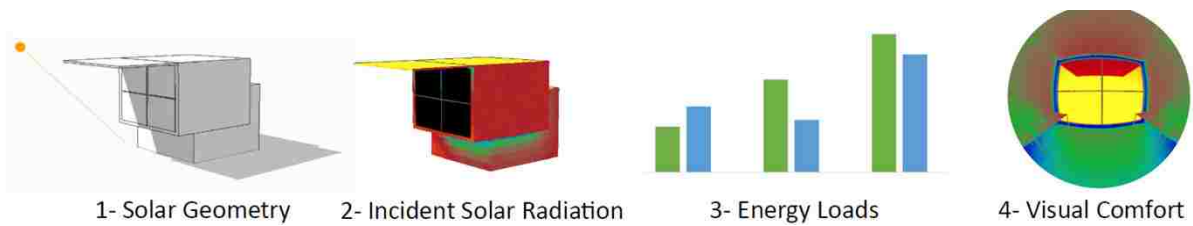
The setting for the illustration model is a 6m x 6m (20 ft. x 20 ft.) south facing office with a window dimensions of 5m x 3m (Figure 10). The office is located in Seattle. South orientation was chosen to study the impact of shading devices throughout the day (East and West facing facades have much shorter periods of sun exposure). This office was modeled in Rhino and exported to various software including Ecotect (Robert A, Marsh AJ, 2001) and DIVA (http://solemma.net/Diva.html) utilizing simulation engines such as Radiance (https://www.radiance-online.org/) and Energy+ (https://energyplus.net/) for solar, shading, thermal and daylighting analyses.

Figure 10: Rhino rendered model and plan.

2.1 SHADING DESIGNS BASED ON SOLAR GEOMETRY

In this technique, the designer applies cut-off dates and time for a given orientation to develop the geometry of a shading system. The basic premise is to allow solar radiation to reach to the window or the façade during the heating season (allowing passive solar heating) and to provide shading during the cooling season. The cut-off dates delimit the heating and cooling seasons, or more generically they divide the year into two, when a shading is desired or not. Based on the cyclical movement of the sun in the sky, four key dates are given in Table 1. A generic cut-off date and time can be specified between spring and autumn equinoxes (March 21 – September 21) between 8:00 am and 5:00 pm.

NAME	NTH.HEM.	STH.HEM.	DESCRIPTION
Summer Solstice	22 Jun.	22 Dec.	Sun at its highest altitude
Autumn Equinox	21 Sep.	21 Mar.	Sun rises due east, sets due west
Winter Solstice	21 Dec.	21 Jun.	Sun at its lowest altitude
Spring Equinox	21 Mar.	21 Sep.	Sun rises due east, sets due west

Table 1 - Important dates relevant to solar position.

A more refined approach incorporates the processing of annual climate data to identify the heating and cooling degree periods (Olgyay and Olgyay 1957, Shaviv 1975, Etzion 1992, Arumi-Noe 1996, Kabre 1999).
This technique is simple enough to be applied through manual methods, but computerized approaches allows the utilization of ray tracing and solar vector algorithms for quicker results. The resultant optimized shading forms are derived from the datelines and analemma of a sun path diagram in a given location (Marsch 2003, 2005).
Shading devices can be designed in many shapes and forms. The most commonly used devices are given in (Figure 11):
      1. Overhangs and louvers
      2. Fins
      3. Louvers
      4. Blinds
      5. Eggcrates
      6. Perforated screens
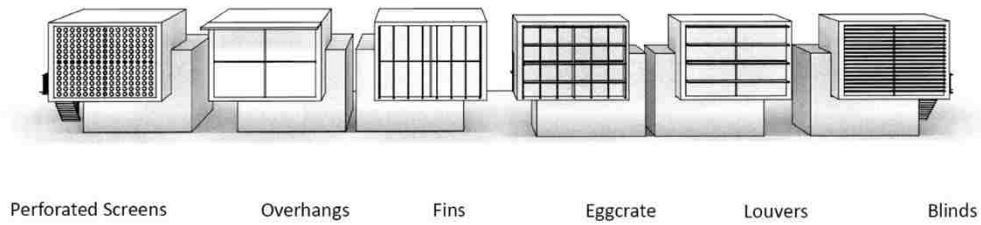
Figure 11: From left to right: Overhang-Gibraltar Airport by Blur Architecture and 3DReid, Louvers- Aqua was designed by Jeanne Gang, Fins-Asakusa Culture Tourist Information Center, Eggcrate-The Chandigarh High Court, Perforated Screen- Social Facilities in Roses by Exe arquitectura.

In order to illustrate the solar geometry based shading system design, Ecotect software is utilized. Although Ecotect is defunct at this point, some of the capabilities on shading device design are useful for discussions on the topic. Figure 12 illustrates the stereographic sun path diagram for the study model. Sun-path diagrams are a 2D representation of the annual movement of the Sun through the sky. The path of the sun at different times of the year is then projected onto this flattened hemisphere.

Without any shading device and neighboring structures, the south facing office receives direct sunlight almost throughout the entire year. The horizontal arcs are the datelines, and the 8-figure analemmas are the hour lines; collectively they illustrate the movement of the sun throughout the year for Seattle (47° N Latitude). The shaded area represents the shading from the surrounding walls in the studied model.
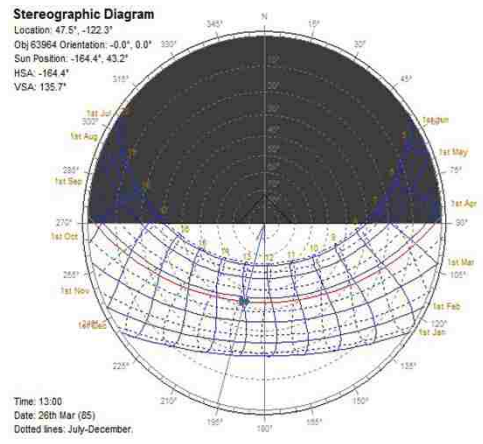
Figure 12: Sun path diagram without any shading devices

2.1.1 Overhangs

A window overhang is a horizontal surface that is placed over the window. Overhangs and other horizontal shading devices (such as louvers and blinds) are used particularly to shade southern exposures as they are effective to provide shading for the high altitude sun in the sky.

The optimized shading device wizard in Ecotect reverse engineers the process of designing a shade. It projects the window towards the sun at a particular time to determine the optimum shape for the shade and its best location, instead of first designing the shade and then measuring the effectiveness of it. The intersection of this with the shading plane forms the projected profile of the window. This process is repeated for each hour of the day. For this model, a shading device is generated using the cut-off dates from March 21st to September 21st during office hours from 8:00 am to 5:00 pm (Figure 13a). The overhang blocks sunlight entering through the glass surface in the assigned period. The program can generate a binary result as shown in (Figure 13b). The blue area is the shade from the overhang, and covers the dates and times of the year where at least 50% of the window is shaded. If the overhang is shading less than 50% of the window surface, it is interpreted as non-shaded (shown in white). Figure 13 c illustrates a refined analysis of the shading capabilities of the same overhang. The legend illustrates the percentage of the window surface that is shaded by the overhang in a given date and time. A white color denotes that 0% of the window area is shaded, a black color denotes that 100% of the window area is shaded, and the tone of the gray reveals the percentage of the window area that is shaded by the overhang as quantified in the legend.
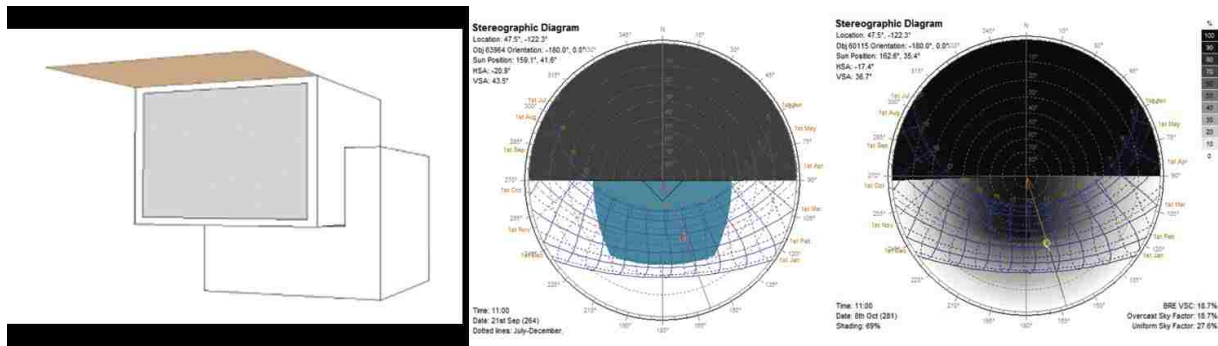
Figure 13.   **a)** Optimized overhang generated by Ecotect   **b)** Sun path Diagram   **c)** Sun path shading percentage Diagram

The automated design of the overhang is partially successful. It blocks direct sunlight for the assigned period. However, it can be observed from the 50% shading diagram that it overshadows beyond the cut-off dates, and it under shadows in between the cut-off times. Moreover, it is a large cantilever which poses structural challenges. Its dimensions are 4mx6m (13ft x 20ft); it is almost the same size as the floor plan. Instead of utilizing one large shading device, it is possible to break into many smaller size elements. Such examples include louvers and venetian blinds.
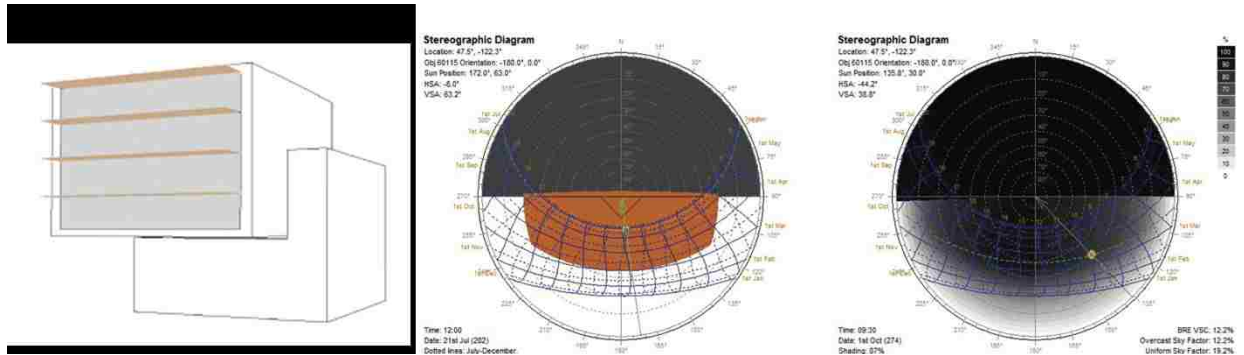
Figure 14: Manually generated louvers

The sun path diagram in Figure 14 demonstrates the shading capability of the horizontal louvers. It is clearly seen that the louvers provide better control over the shading period, where the 50% shade line aligns well with the cut-off dates of September 21st and March 21st, and the shading period throughout the day is longer. The shading device is structurally more feasible, and the number and the depth of the system are design variables. The example in Figure 15 utilizes the same concept of horizontal shading device with a different depth and slat count. The shading outcome is quite similar.
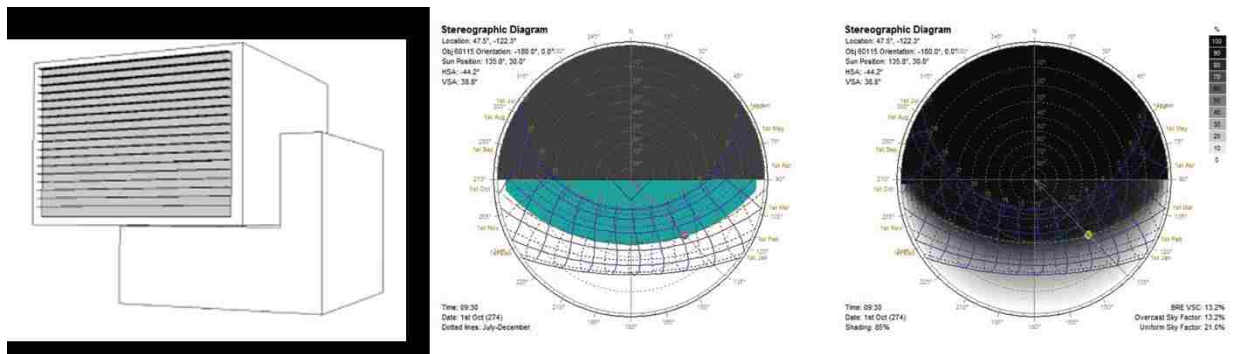
Figure 15: Manually generated blinds.

2.1.2 FINS

Fins are vertical shading devices and they are most effective in the East and West orientations. They block the direct sun rays when the sun in low and oblique. For the South facing window (Figure 16), fins can only be useful during the early morning and late afternoon hours.
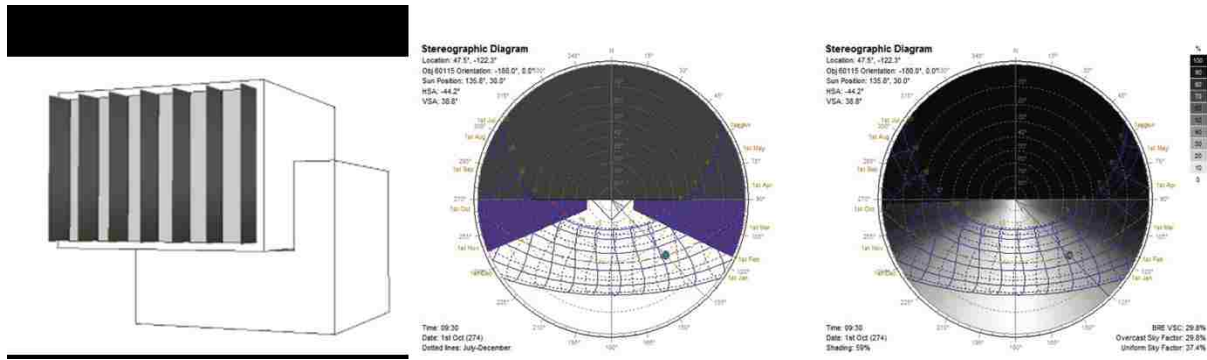
Figure 16: Manually generated Fins to block early morning and late afternoon sun on a south facing facade.

2.1.3. Eggcrate:

Eggcrates are the combination of horizontal and vertical shades. From the sun path diagram (Figure 17) it is clearly seen that the horizontal shades (orange) are more effective than the vertical shades (purple) for a south facing window. Eggcrates are rigid structures and they are utilized only in extreme hot climates. Instead, perforated screens or other integrated facade elements are more commonly seen in contemporary architecture.
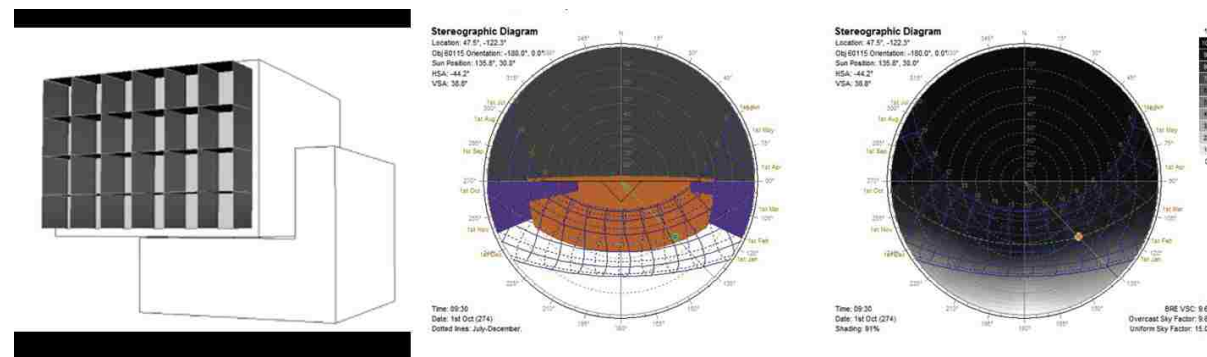
Figure 17: Rigid eggcrate structure that consist of both fins and louvers.

2.1.4. PERFORATED SCREENS

Early examples of perforated screens (Mashrabiya) can be found especially in eastern architecture (such as the Persian geometric ornamentation patterns). These screens are fixed exterior panels that provides shading to the facade, and privacy to the interior, while allowing air movement around the structure.

The modern uses of these screens reveal the connection to the past and how oriental and vernacular cultures are being reproduced (Figure 18).

Figure 18 Perforated screens (Mashrabiya) from Traditional to Modern.
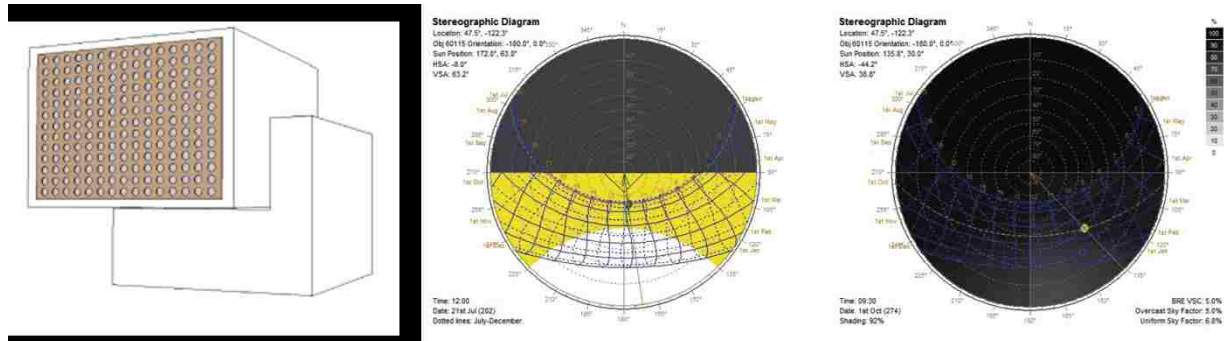
Figure 19: Perforated screen generated in Grasshopper and baked into Rhino

In Figure 19, a screen with perforated circle apertures is evaluated. The diameters of the circles are .2m (7.8 inches) and the opening to opaque ratio is 3:4. The shaded area in the sun path diagram (Figure 19) is similar to the eggcrate shade. It provides shading throughout the year. It is important to note that the maximum resolution of the sky subdivision allowed in this analysis is 2° (which is a software limitation), and it does not have enough resolution to demonstrate the light and shadow patterns from the perforation. A rendering with high number of rays traced into the scene is warranted to evaluate the actual performance of this shading device (it is discussed in Section 2.3 and demonstrated in Figures 32, and 33).

Sky dome subdivision is dividing up the sky into small segments, illuminance or irradiance zones. Figure 20 shows a range of different sky subdivision strategies. Tregenza suggested that the optimum diameter of a sky zone was a cone opening approximately (10.15°) (Tregenza, 1987). Based on his suggestion, the CIE -Commission Internationale de l'Eclairage- recommended the use of a 145-segment equal-area subdivision based on 8 equal altitude bands which allows each zone to be considered as approximating a point source (CIE, 1989). The ESP-R utilized a similar approach but in larger cone opening of 13.39°. Both of these sky segments either do not fulfill the sky or overlaps. Daysim covers the complete hemisphere (Reinhart et al., 2001). Different sky resolutions that include 578 and 2305 are proposed and adopted in various software and methodologies (Reinhart et al, 2001).

(a) Tregenza   (b) ESP-R   (c) DAYSIM
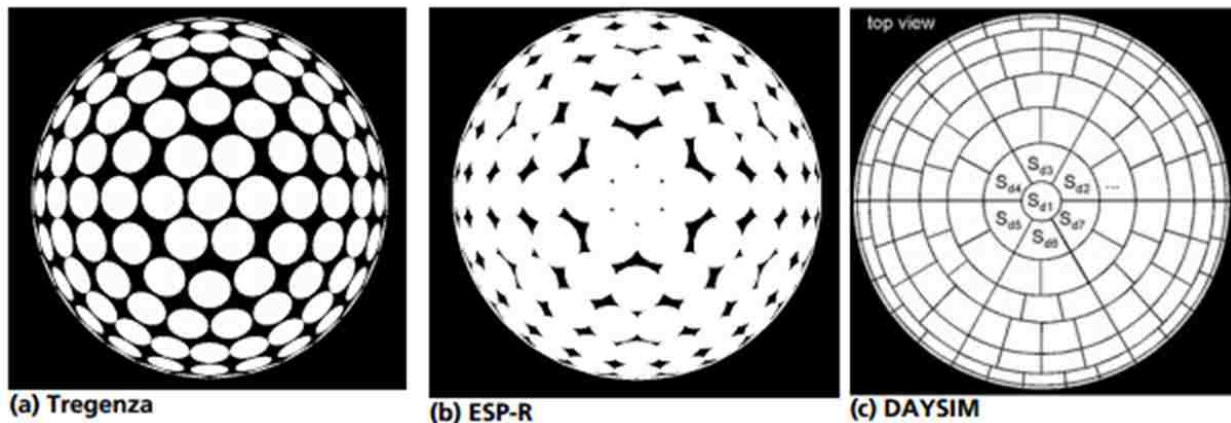
Figure 20: Some examples of different approaches to sky subdivision.

For a quicker calculation, Ecotect uses a simple latitude/longitude method in which the sky is divided into vertical segment (altitude angles) and radial slices (azimuth lines) (Figure 21).

The minimum number of sky subdivision consist of 5 °by 5° spherical grid that gives a total of 1296 segments (72 x 18), and the maximum number of sky subdivision divisions include a 2° by 2° spherical grid that gives 8100 segments (180 x 45) which seem more accurate (Marsh, 2007). However, in the previous analysis, this seems inadequate and requires a finer sky division with a higher resolution to illustrate the effectiveness of the perforated screen.
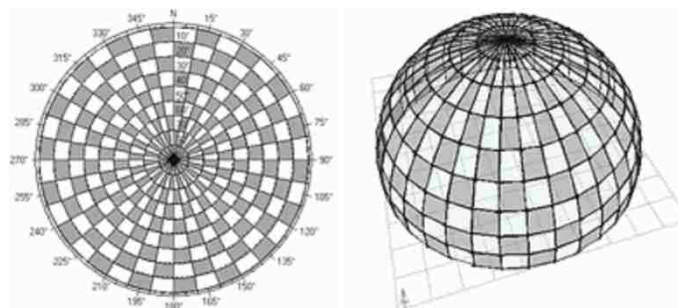
Figure 21 Ecotect sky dome subdivision of 10 degrees.

2.1.5 EVALUATION OF SHADING DESIGNS BASED ON SOLAR GEOMETRY

Designing shading devices based on solar geometry is an oversimplified methodology. The only data that is processed in this methodology are the latitude of the location and the orientation of the window surface. The position of the sun in the sky for a given date and time is calculated, and the shading device form and size are determined based on the sun position at the cut-off dates and times. Another limitation is that the weather and climatic conditions are not processed, and it is assumed that the sky is clear throughout the year. It is obvious that these assumptions are not realistic. Figure 22 demonstrates the overhang generated for an office in Quebec City. Seattle and Quebec City are located on the same latitude (47.6°N and 46.8°N, respectively); therefore, the sun path diagrams for both cities are quite similar. However, the climates are very different. Since only latitude and orientation was the only input, this methodology yield to same shading devices in two cities that have very different climates, and therefore, very different performance needs. Studying the weather data and selecting different cut-off dates based on heating and cooling requirement would provide improvements to the performance of shading devices, yet the oversimplification persists as the methodology ignores atmospheric conditions such as cloud cover, air pollution, and atmospheric turbidity. The actual amount of direct and diffuse solar radiation is not studied. There is another significant shortcoming in this methodology. In automated methods demonstrated above, the impact of surrounding structures is not considered. Although this impact could be added by manual calculations, it is a tedious and long process, therefore it is usually not practiced. In dense urban layouts, the shading from surrounding structures should be carefully considered as an important factor on façade design. Software like Ecotect can generate optimized shading systems based on cut off dates, but a significant downside of this approach is that these automatically generated shading devices can provide shadowing during the periods of the year when it is undesirable to shade (Sargent et al, 2011). The next section discusses the shading design strategies that encompass weather data and surrounding context.
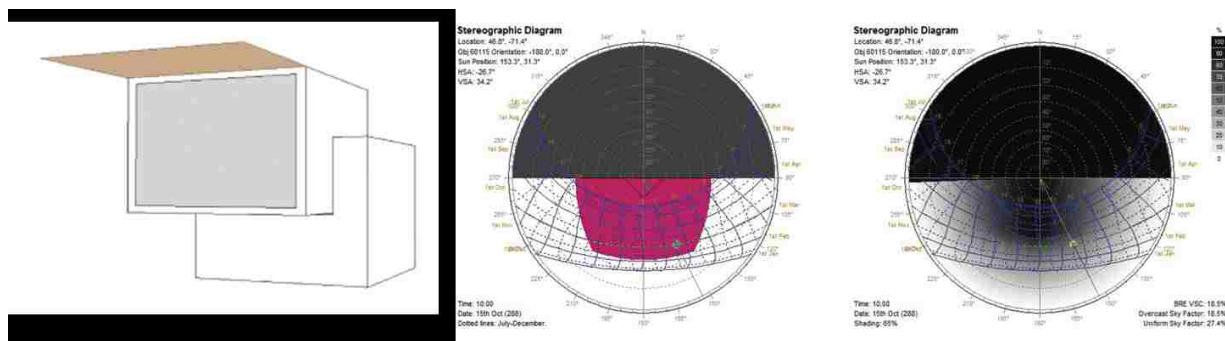
Figure 22: Shade and sun path diagram for Quebec City in Canada.

2.2 SHADING DESIGNS BASED ON INCIDENT SOLAR RADIATION (INSOLATION)

The second technique that is used to shape shading devices is based on calculating the amount of the solar radiation falling onto a surface (window). Incident solar radiation, insolation in short, is the amount of direct and diffuse solar energy that falls on a surface. Typically, high levels of solar radiation are not desirable in summer as it will increase the cooling loads; and it may be desirable in winter as a passive solar strategy. This strategy differs from the previous strategy as it is not only considering the position of the sun in the sky, but it incorporates hourly variations of weather data (direct and diffuse components of solar radiation as a result of cloud cover and turbidity), along with the obstructions and reflections from the neighboring buildings. As a result, shading device is optimized for a given location.

Generating annual radiation map on a building or an urban fabric can provide analytical means of protection against solar exposures. However, the production of such output is time consuming and computationally expensive.
Design tools use different approaches to create these types of results. Ecotect uses the grid method which generates a grid on the window to calculate and determine the overall shading importance of each cell (Kaftan et al. 2005). RADIANCE, a popular ray-tracing based lighting simulation and visualization program, generates a cumulative sky and produces these maps based on a given climate file. RADIANCE software, without a graphic user interface, is well-suited to programmers and people with a high degree of computer proficiency. The interface is command-based in a fashion that is familiar to UNIX users, but challenging for many who are used to the menus and point-and-click interfaces of modern software. However components including GenCumulativeSky are available through user-friendly softwares like Diva, Daysim, HoneyBee and Ladybug that utilize RADIANCE as their simulation engine.

The methods discuss above has been utilized to compute the insolation levels on the proposed model.

2.2.1 OVERHANGS WITH INSOLATION ANALYSIS

An insolation analysis for the overhang designed in Section 2.1 for Seattle and Quebec City is given in Figures 22. The comparisons incorporate the impact of location, weather data, surrounding geometry and materials on the insolation levels. This method is based on generating a grid over the shading device, and direct and diffuse solar radiation is calculated on the grid. Parts of the grid that reveals high levels of solar radiation can be utilized as parts of the shading device that are more instrumental in controlling the solar energy; therefore, affords the designer to reshape the shading device by eliminating the low impact grid cells. Figures 24 also demonstrates the impact of the material of the surrounding buildings on insolation levels. Surrounding buildings not only block certain parts of the sky and provide shading to the studied building, but they also reflect light. A mix of opaque and glazed facades surrounds the studied offices are simulated and each combination has a different effect on the amount of energy falling on the optimized shade. The impact of materials has become a particularly important aspect of solar analysis as more and more use of highly reflective building materials can cause significant problems to the neighboring buildings. It is evident that insolation based shading devices are more realistic, as they can result in different shading devices for different climates and different sites with within the same climate.

In the analysis below, shading devices were analyzed using insolation analysis over a grid. Point cloud ray-tracing approaches and grid method approaches were the first examples that demonstrated the idea of using insolation to shape shading devices, and these methods are incorporated into Ecotect (Marsh 2003, 2005, Kaftan and Marsh,2005).
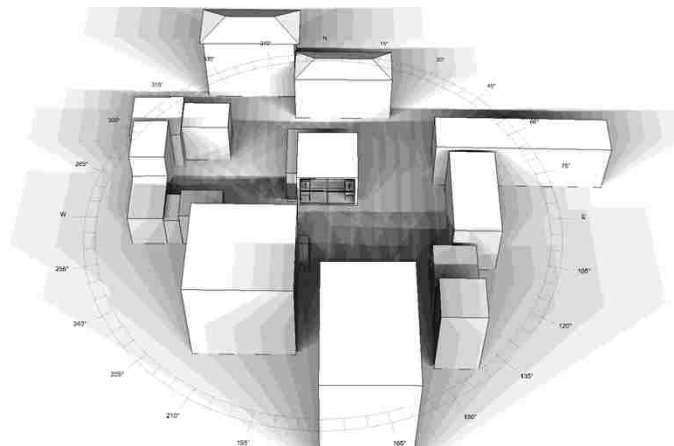
Figure 23: Office model surrounded by a mix of opaque and glazed buildings to study the impact of the materials on insolation levels.
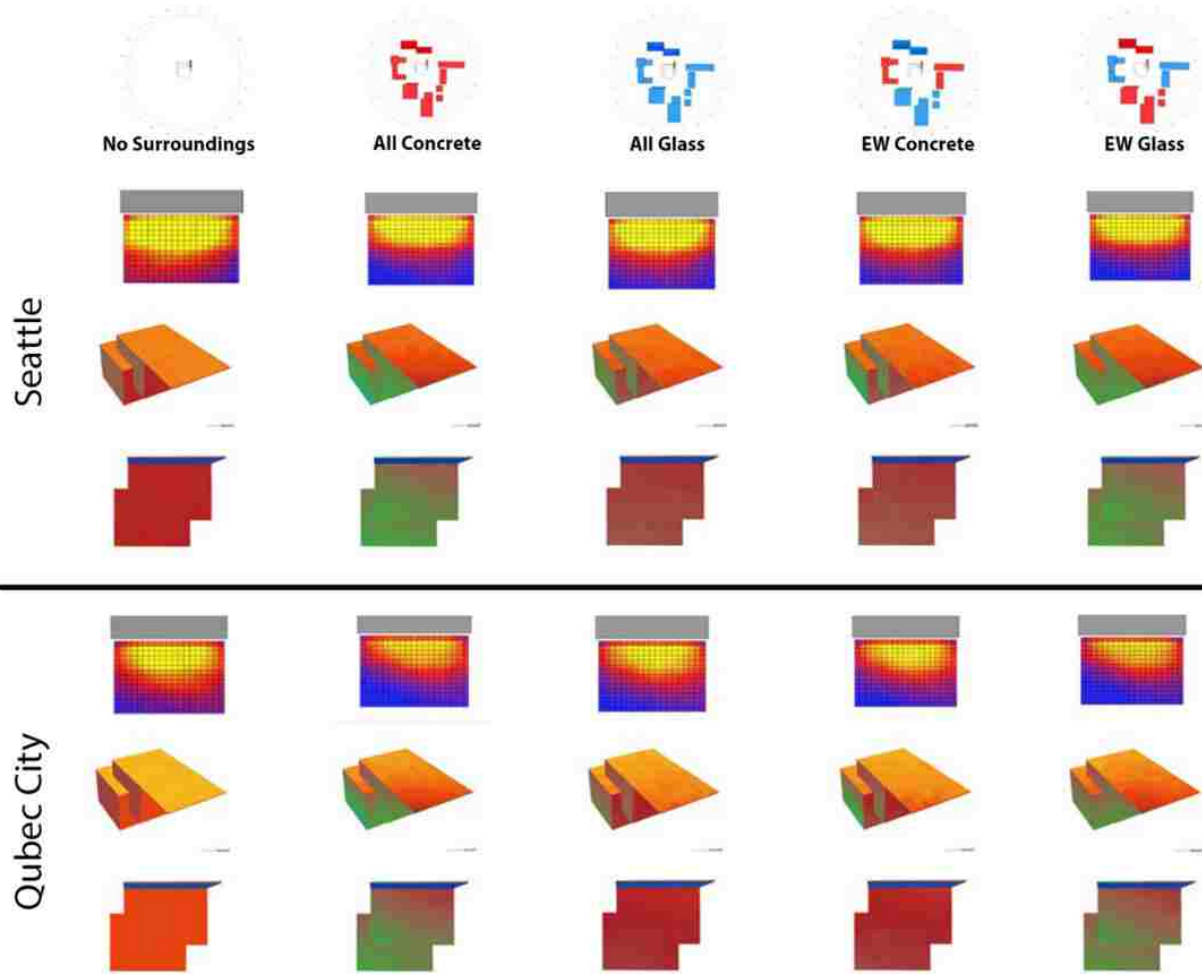
Figure 24: Top row: Total incident solar radiation falling on the overhang for Seattle and Quebec City using Ecotect.
Bottom row: Annual Solar radiation effect on the proposed office with different surrounding materials.

The insolation study shown in Figure 24 bottom row, employs Robinson and Stone's computation method (2004) embedded in Diva. This method harnesses a Radiance module called GenCumulativeSky to create a continuous cumulative sky radiance distribution. This cumulative sky is then used in a Radiance backwards ray-trace simulation.

The close-up simulation in figure 26 shows the difference between Seattle and Quebec City with a lower limit of solar radiant exposure of 1000 kwh/m2. This diagram shows the solar radiation in Quebec City is more intense than in Seattle. The results obtained are compared with Ecotect insolation results, and it's clearly seen that with all concrete surrounding and with the direct and diffuse sunlight, Diva simulations are more accurate. The reason behind the difference in results is RADIANCE. RADIANCE processes direct and diffuse solar irradiance images and provides output that is rich in statistical information (Robinson and Stone, 2004).

Seattle, WA 47.6062° N   Quebec city,Canada 46.8139° N

0 ▬▬▬▬▬▬▬▬ 1350
Solar Radiant Exposure [KWh/m2]
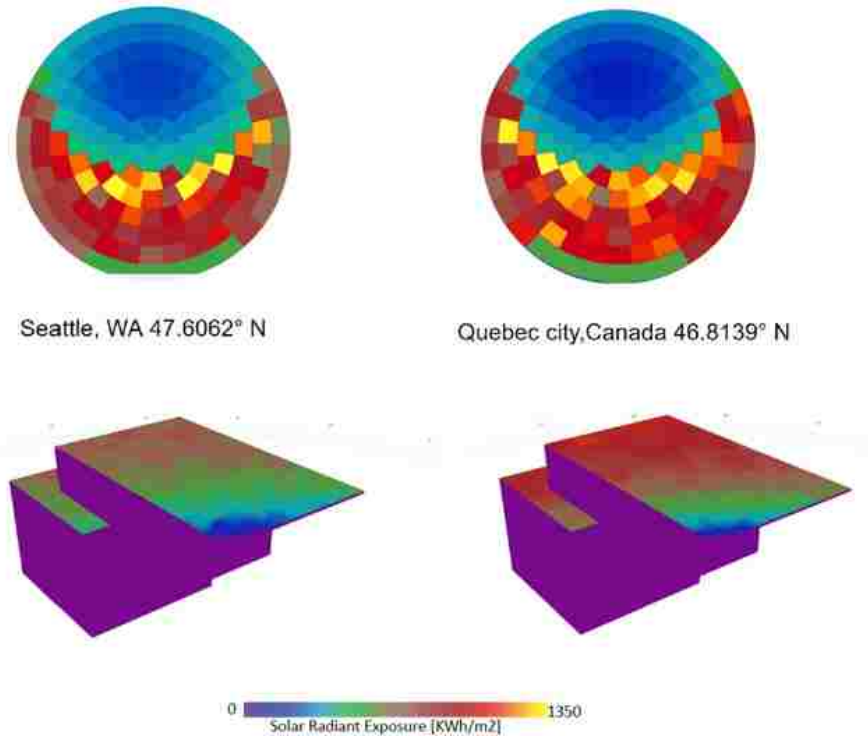
Figure 25 : Top: Annual Radiation sky subdivision for Seattle and Quebec City
          Bottom: A close-up of the Annual Solar radiation effect on the proposed office with concrete surrounding.

Seattle RADIANCE   Seattle DAYSIM

All concrete

1000   1350
Solar Radiant Exposure [kWh/m2] ▬▬▬▬
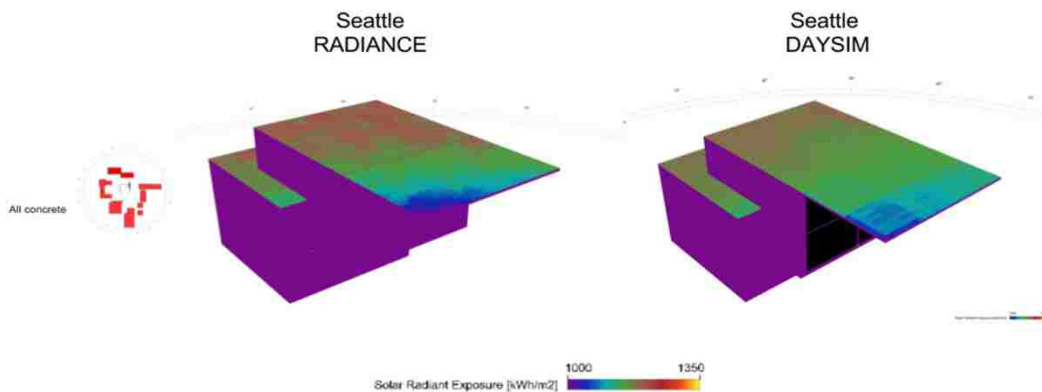
Figure 26: The difference between Radiance and Daysim: Radiance uses accumulative data whereas Daysim uses hourly data.

www.manaraa.com

The GenCumulativeSky simply divides the sky vault using Tregenza sky subdivision in which each of 145 patches has an equal area of distribution. The Perez all weather luminance distribution model is then used to predict the luminance / radiance at the centroid of these patches and the results are accumulated for the period of interest (Robinson and Stone, 2004). In Figure 26 two GenCumulativeSky were generated to compare the radiation falling from the sky. The results obtained show more radiation towards the south and south west of Quebec City. However, it is more concentrated towards the South in Seattle. The cumulative sky radiances in Seattle and Quebec City align with the results from the Radiance and Daysim, but the results from Ecotect provide odd results where the insolation levels are higher in Seattle than Quebec City.

2.2.2 EVALUATION OF SHADING DEVICES BASED ON INSOLATION

Insolation based shading device design is a better way of shaping shading geometry, in comparison to methods based solely on solar geometry. The impact of weather conditions and the occlusion and reflection of solar energy from the surrounding urban fabric and forestry can be modeled and incorporated into developing a more robust optimum shading device. However, this approach is also reductionist as the analysis is restricted to the façade level, and does not address the environmental and spatial characteristics of the space behind that façade. The next section discusses the shading design strategies that encompass studying the heating and cooling loads for a given thermal zone behind the façade to shape and size a shading device.

2.3 SHADING DESIGNS BASED ON HEATING AND COOLING LOADS (THERMAL ANALYSIS)

The façade is one of the most significant contributors to the energy consumption and the comfort parameter of any building. The necessary steps on ensuring that the environmental factors and energy efficiency strategies are integrated within the design process. High performance façades need to block adverse external environmental effects and maintain internal comfort conditions with minimum energy consumption. In this case location and climate become crucial factors in selecting the appropriate design strategies.
This section discusses different building performance analysis steps that can assist in the design process, such as energy modeling and thermal comfort modeling.

Thermal comfort is defined as "the condition of mind which expresses satisfaction with the thermal environments" (ASHARE,2004). It is a subjective measurement since it relies on the air temperature, humidity, radiant temperature, air velocity, metabolic rates, and clothing levels and each individual may experience these sensations differently based on his or her physiology and state (Huizenga et al., 2006).

Thermal comfort is calculated as a heat transfer energy balance. Heat transfer through radiation, convection, and conduction are balanced against the occupant's metabolic rate. The heat transfer occurs between the environment and the human body, which has an average area of 19 ft2. If the heat leaving the occupant is greater than the heat entering the occupant, the thermal perception is "cold." If the heat entering the occupant is greater than the heat leaving the occupant, the thermal perception is "warm" or "hot" (Autodesk, sustainability workshop).

Similarly, thermal comfort can be quantified to determine the shape of a shading device. The choice of facade glazing materials influences occupants' thermal comfort (Huizenga et al., 2006). The impact may be different for summer and winter. During winter, the thermal comfort is largely driven by inside window surface temperature, which is usually colder than the other surfaces inside the room. During the summer, thermal comfort is driven by the combination of the inside surface temperature of the glass and the transmitted solar radiation through the glass. These in turn are significantly influenced by the construction of the glazing units, the material properties of the glass, and the effectiveness of shading elements used with the window. Thus, a comprehensive thermal analysis used to determine an optimum shape is would reflect a higher level of realism considering of the thermal properties of a given space (Aksamija, 2013).

It has become important that designers evaluate building energy performance at early and schematic project phases before a detailed energy model is produced. This saves the project from drastic changes due to misguided energy goals.

There are varieties of tools and simulation programs with different modeling capabilities. Crawley at al. published a study that compared capabilities of twenty different building performance simulation programs some of them are still used nowadays (BLAST, BSim, DeSTm DOE-2.1E, Ecotect, Ener-Win, Energy Express, Energy-10, EnergyPlus, eQuest, ESP-r, IDA ICE, IES VE, HAP, HEED, PowerDomus, Sunrel, TAS, TRACE, TRYNSYS) (2006). These tools are used with varying degrees in architectural practices. There are two main simulation engines, namely DOE2 and Energy+. Figure 27, 28 shows a brief history of the development of the simulation engines, and the software that utilizes these engines particularly among architects.
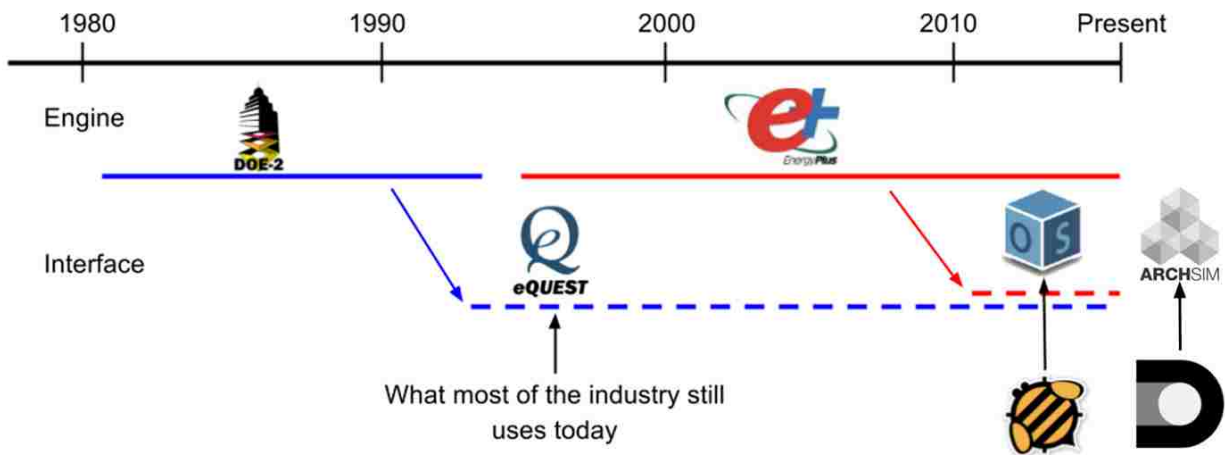
Figure 27: History of used building performance simulation programs.

	Solar analysis	Shading Masks	Energy Modeling	Daylighting	Insolation
Radiance				✓	
Energy Plus			✓		
Ecotect	✓	✓	Limited	✓	✓
Diva (Archsim)	✓		✓	✓	✓
LadyBug HoneyBee	✓	✓	✓	✓	✓

Figure 28: Building performance simulation software programs and their applicability for facade design.

Figure 28 provides an overview of applicable simulation programs for the design of sustainable, high-performance building facades. Since there is not a single simulation program that can address all aspects and design questions that are posed during the design of high performance facades, typically several different programs must be used to investigate properties and behavior of facade systems. The figure shows which applications are suitable for these types of performance simulations, and their applicability for specific design aspects.

The cutoff dates utilized in solar geometry based shading devices aim to provide shading during the warm seasons, and to allow sun penetration during the cold seasons, it stands to reason to utilize heating and cooling loads of a space to shape a shading device. Therefore, energy usage and/or thermal comfort can be used as criteria to develop an optimum shade form. The cellular method (Marsh, 2005) and SHADERADE (Sargent et al., 2011) developed a methodology to utilize thermal simulations (Energy+) to study individual shade elements (cellular object) to derive an optimum shading device. This approach incorporates the impact of outdoor conditions (such as the position of the of the sun, weather, and surrounding buildings) along with the impact of internal characteristics of the thermal zone behind the façade to design a shading element. The size of the thermal zone, set points, internal loads (such as number of people, lighting loads and equipment loads), and material properties are processed to evaluate the shading needs of a given space. This is done by generating a grid of cells over a window, and the simulation determines the contribution of each cell on the resultant heating and cooling load.

Different software such as COMFEN [https://windows.lbl.gov/software/comfen/comfen.html], DIVA [http://solemma.net/Diva.html], ARCHSIM [http://archsim.com/] can be utilized to model the thermal properties of a space. These software utilize Energy+ [https://energyplus.net/] as a simulation engine.
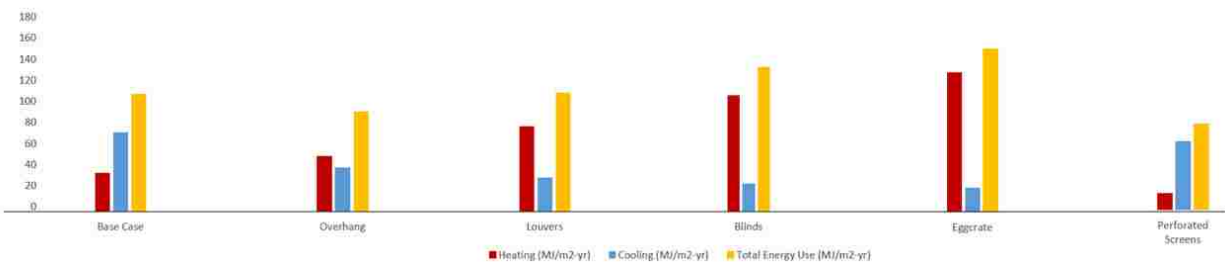
Figure 29: Comparing heating and cooling loads for different types of shades in Seattle

In the example given here, the five proposed shading devices were compared for two different office depths for energy usage with Comfen. In general, the application of shading device is expected to raise the heating loads, and lower the cooling loads.

Figure 29 shows that the base case scenario without any shading devices has a moderate amount of energy usage and once a shading device is applied a reduction in the heating gain is evident. The overhang shade typically just blocks direct sunrays, the louvers and venetian blinds both block direct and diffused sunrays. The peak energy values is evident in The eggcrate in the 6x6 room depth. The mesh or perforated screen is performing much better because it acts like an insulation by creating static air between the window and the outside

The annual average thermal comfort chart shows that almost 100% of the year occupants are comfortable in the office with the perforated screen and it has the lowest energy usage of all five shades. The rest of the shades have slight differences; however, the mesh uses the least heating loads and the eggcrate, louvers and venetian blinds uses the most heating and cooling loads.

2.3.1 EVALUATION OF SHADING DEVICES BASED ON THERMAL LOAD

Thermal analysis of a thermal zone behind a shading device is a comprehensive analysis, and provide significant advancement compared to the two techniques discussed before. However, there is another component that is relevant in operation of shading devices. The impact of daylighting is discussed in the next section.

2.4 SHADING DESIGNS BASED ON DAYLIGHTING CONTROLS

The sun is the source of all daylight and the sky appears to be self-illuminating by the scatter of air, water vapor, and dust. The illumination produced by the sky varies depending on seasonal and geometrical parameters. Sky models allow us to model sky luminance distributions.

Scientist have been monitoring the sky luminance distributions since 1950s. The basic daylight components usually contain hourly integrated values of global and diffuse irradiance (Larson et al,2003) (Figure 30).
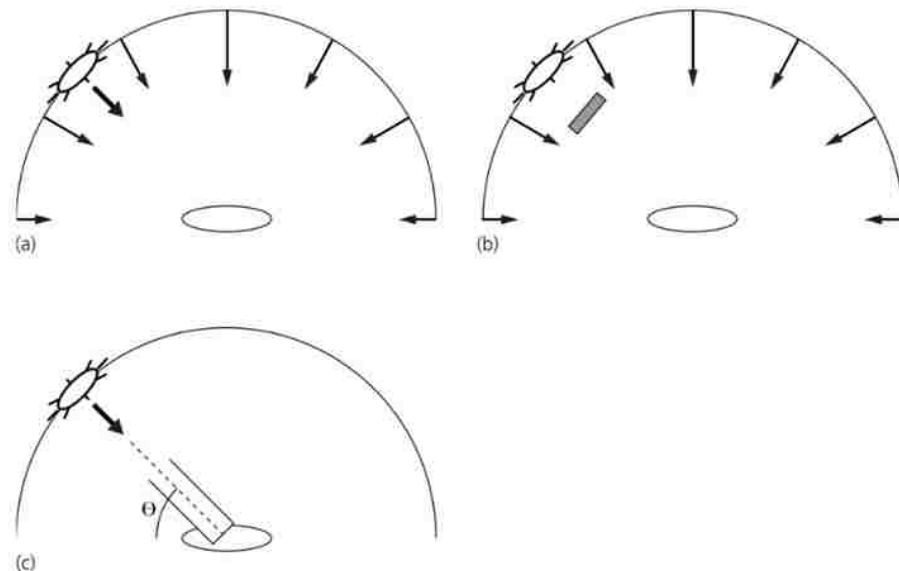
Figures 30: Basic daylight components: a) global horizontal (sky and sun), b) diffuse horizontal (sky only), and c) direct normal (sun only).

Latitude, water mass, cloud cover and turbidity have a impact on the sky model and its luminance which impact daylight simulation (Larson, 2011)The three types of sky models utilized in the available software are categorized here as (Inanici, Liu, 2016):

1-CIE models:
> They are mathmatical model that calculate the avarage sky brightness and provide the best fit model for daylight measurements. Most commenly used CIE skies are: Clear, overcast and Intermediate skies.

2-Perez All weather models:
> Perez models represent luminance distrubutions for direct and diffuseed horizontal irradiance. They are commonly used for annual daylight simulations.

3-Image based models:
> Also called "HDR" -high dynamic range- fisheye images of the sky dome. This method os used for capturing the cloud distrubution and the circumsolar region.

Figure 31 visualizes the sky models for Seattle and Quebec city for June 21 at noon. These simulations show the intensity of the luminace in the sky. An overcast sky provides a symmetric lumianance distribution on each orientation, but the zenith is 3 times brighter than the horizon. Seattle and Quebec city have the same intensity in a CIE sky definitions as they share the same lattitude. However, differences in perez sky are expected dur to the different direct and diffuse radiations in the weather data file.
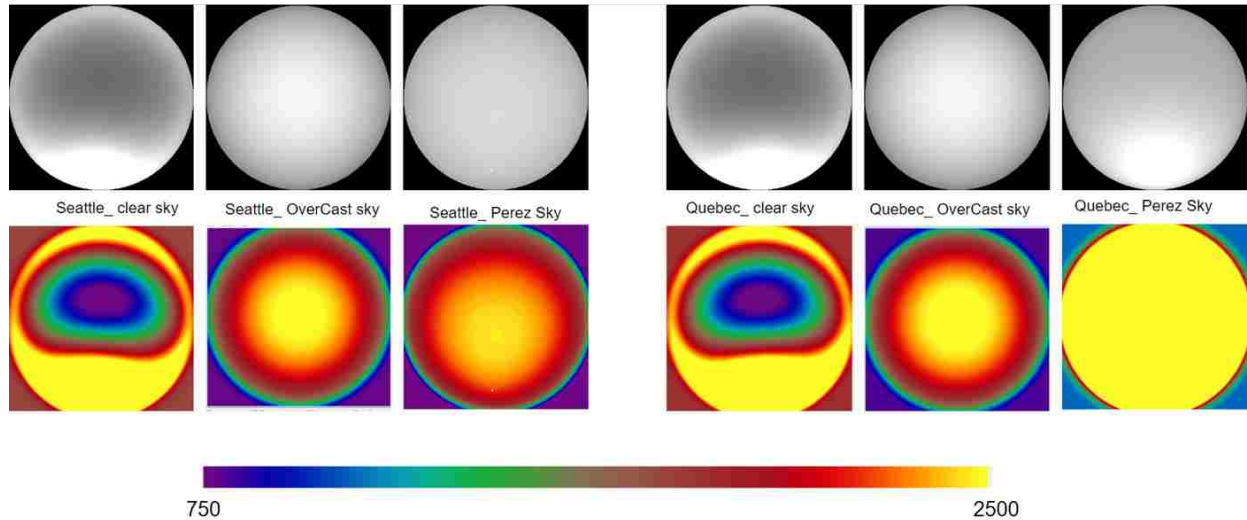
Lighting alone takes up around 15% of total building energy consumption (Pérez-Lombard, 2008). Therefore, architects and engineers are actively looking for solutions to reduce lighting energy. Beside energy issues, lighting plays a significant role in occupants' comfort and satisfaction levels (Boubekri et al.,1991).

Inside a building, access to daylight makes the indoor environment healthier and more comfortable for occupants; natural lighting is also linked with greater productivity (Boubekri,2008). When designed with proper glare control and minimized solar heat gain, daylighting provides high-quality light while significantly reducing energy consumption for lighting and cooling. An effective facade shading design should contribute to the creation of such an environment that will reduce building energy expenditure and optimize daylight distribution.

Shading devices impact both visual and thermal comfort of the interior. They have been designed based on thermal analysis, however, many studies show that the most common reason for operating shading devices is visual comfort, i.e. glare (Innoue et al. 1998, Lindsay and Littlefair 1992; Littlefair 2002; Inkarojrit 2007, van den Wymelenberg 2012). For that reason, controlling daylight should be the most dominant approach to designing shading devices .

Therefore, it stands to reason to design shading devices based on daylighting and visual comfort criteria. When considering daylight and visual comfort, designers need to consider illumination levels, daylight distribution, and protection against direct sunlight and glare. Sustainable strategies for improving natural light levels provide ways of increasing that depth without increasing the amount of glazing (Aksamija, 2013)

The available daylighting metric and simulation capabilities are illustrated here, using Diva-for-Rhino which is highly optimized daylighting and energy modeling plugin for Rhino is utilized for daylighting simulation. The simulation in Diva is based on powerful environmental performance engines including Radiance, Daysim and EnergyPlus. Three metrics are selected in this study to study the impact of shading devices: 1) Useful daylight Illuminances (UDI); 2) LEEDv4 criteria sDA and ASE; and 3) Daylight Glare Probability (DGP).

Useful Daylight Illuminances (UDI) (Mardaljevic and Nabil in 2005) is a dynamic daylight metric that is also based on work plane Illuminances. Daylight levels are accepted as 'useful' when they are neither too dark (<100lux) or too bright (>3000lux). The upper threshold is meant to detect times that might lead to visual discomfort. The analysis of the space with UDI metric shows the effectiveness of a given shading device; i.e. how it affects the interior lighting conditions. Without any shading device, almost 0% useful light is entering 75% of the space. The light levels are above the 3000 lux threshold, which means it is too glary. The louvers seem to receive highest percentage of useful daylight in the whole office which makes it perform best in terms of daylighting. The perforated screen almost receives good daylight; however, it is clearly seen that it gets too dim at the back of the room.

LEEDv4 (2013) requires that a Spatial daylight Autonomy (sDA300lx,50%) is achieved in 55% along with Annual Sunlight Exposure (ASE1000lx,250h) below 10% of the regularly occupied floor areas (LEED, 2013). Figure 28, shows the overall percentages of the floor area that has a daylight autonomy value of 50% or more. It also shows the annual sunlight exposure (ASE) for more than 250 hours a year that receives over 1000 lux. ASE uses zero ambient bounces, i.e. accounts solely for direct sunlight penetration. This helps in defining the percentage of the over lit areas. Spatial daylight autonomy means that the calculation points in the occupied areas have 300 lux or more 50% of the time. The annual sunlight exposure shows the percentage of light above the threshold. These numbers are high and means that the entire floor plan has both day lit areas and over lit areas. It is clearly seen that a large area of the model is over lit. The UDI shows that short louvers appear to have the highest UDI and performs best in terms of daylighting.

The same analysis was conducted on the same model but with a different depth. From the false color analysis (Figure 32), it is clearly seen that the blinds again have the best performance because it provides stable daylighting in the whole room. Without any shade performs the best towards the end of the room, the eggcrate and perforated screen makes the room darker towards the end.
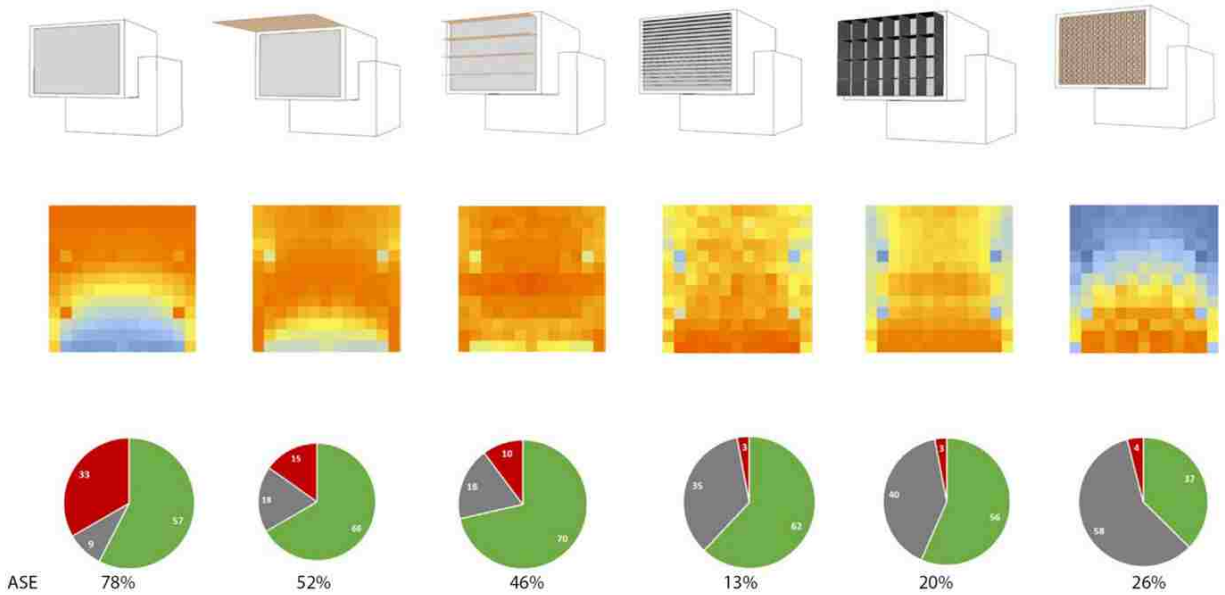
Figure 32: Daylight simulation for the modeled 6x6 office with different shades
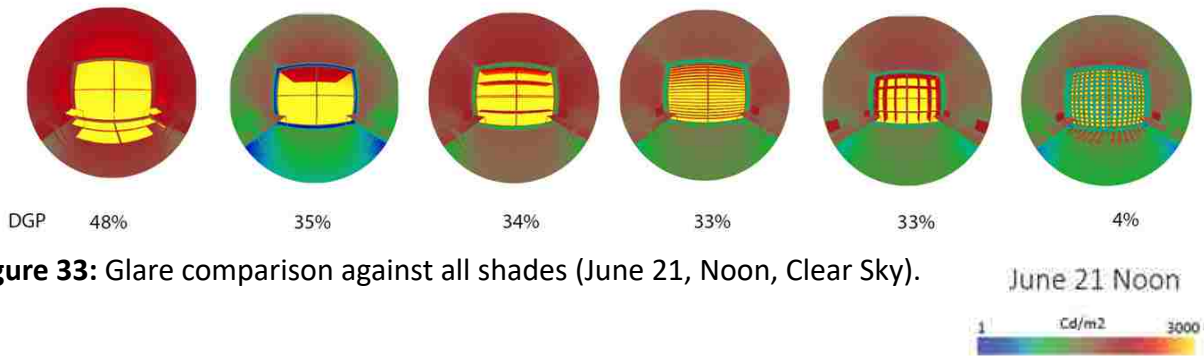
Figure 33: Glare comparison against all shades (June 21, Noon, Clear Sky).

Daylight Glare Probability (DGP) (Wienold and Christoffersen, 2006) represents the percent of people experiencing glare in a given environment.. Like most glare calculations, DGP has two steps; the first step is identifying the potential glare sources with their the size, position and luminance . The second step quantifies the glare index. Figure 33 compares the base case (without a shading device) with all proposed shades for glare. With an evaluation criteria of DGP below 30%, only the perforated screen is effective for the studied date and time. All other shading options provide significant glare problems.

The least percentage of people are disturbed by glare is from the perforated screen and 4% of the pixels are over 3000 cd/m2 which may indicate glare and overlighting. However, in Figure 34, the blinds and louvers perform best and provides the highest UDI.

To sum up, we have a collection of tools and metrics to analyze the daylighting quality of spaces to make decisions on the performance of a given sun screen. However, before employing these techniques, it is necessary to categorize sun screens as static and dynamic. The examples given up to this point are static screens, the next section discusses dynamic (movable) shading devices.

2.5 SHADING DESIGNS BASED ON DYNAMIC SHADING

Daylight is "an interplay of natural light and building form to provide a visually stimulating, healthful, and productive interior environment" (Reinhart C F & Galasiu A, 2006). Given the dynamic nature of daylight, façade design and daylight optimization benefits from a dynamic approach that involves dynamic operations of devices (mechanical systems) and responsive materials. Movable and dynamic shading devices can be utilized to overcome the difficulties in the transition between the indoor and outdoor spaces. Roller shades developed in 1700 and venetian blinds developed in 1760 are considered a manual form of moveable shading devices. Smart materials like electrochromic glass are being used as an alternative to mechanical systems to provide weightless structures that uses less technical assemblies. Few centuries later, responsive facades have been explored with sensors since 1987 in Institute du Monde Arabe building by Jean Novel (Figures 34 -35). Unfortunately, these kinetic structures can be prone to fail and break over time (Khoo and Salim, 2013).

Figure 34: Institute du Monde Arabe building by Jean Novel

Figure 35: Mechanical system for dynamic screen

There a numerous materials and projects that utilize dynamic shading. For example, a Thermo bimetal is a smart material that has many uses in architecture facades. It can be used in shading devices due to its response to sun. (Khoo and Salim, 2013) The Bloom project (Figure 36 by Doris Kim Sung) is an example of a dynamic shading device, which involes 14000 pieces of bimetal to create a shading and proper ventilation when required. The thermo bimetal (Figure 37) curls up in reaction to temperature and allows air to ventilate through the system (Khoo and Salim, 2013).

Figure 36: The Bloom project (Figure 36 by Doris Kim Sung .
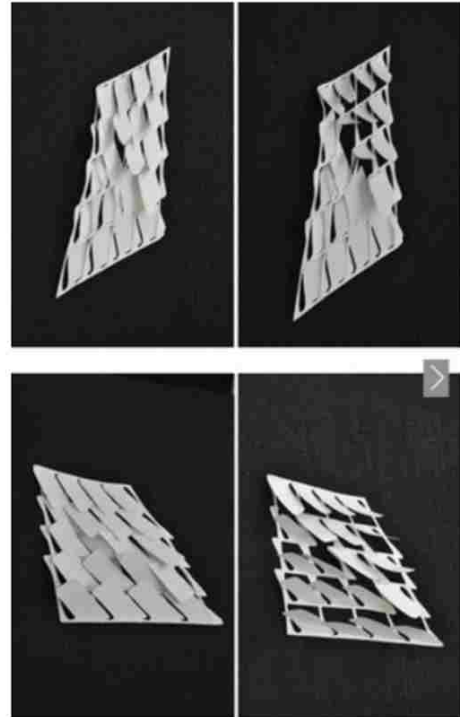
 Figure 37: The Bloom project material and design.

Both materials offer fast and momentary response to the surrounding environment. A responsive facade is a facade that responds automatically to interior and exterior condition to reduce energy consumptions (Roe, 2013), provide occupants comfort and add a pleasant appearance to a space.

Dynamic operation of typical shading devices can be modeled and analyzed in evaluative software. To illustrate the effect of manual and automatic operation of venetian blinds, shade fabric, and electrochromic glass is performed for comparison (Figure 38).
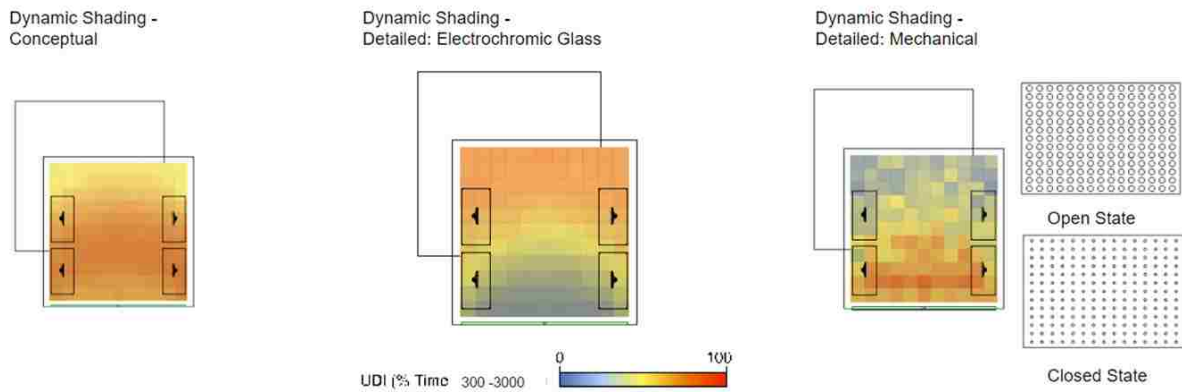
Figure 38: Dynamic shading simulation in Diva
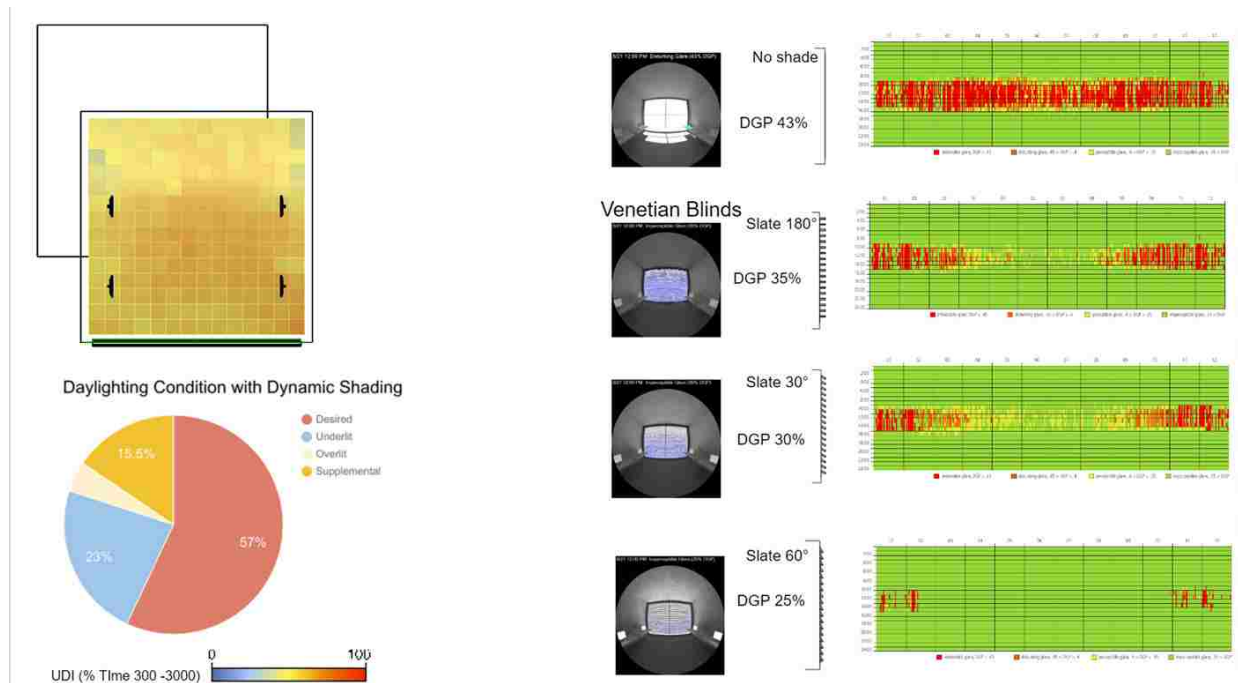
Figure 39: The effect of different angles and slates on the performance of the space

Without shading device: The simulation ran without considering any shading systems. In effect, windows are modeled as 'open' at all times and no blinds or operable shading devices influence the available daylight, even if occupant discomfort might be a problem.

Manual and automatic roller shade: uses translucent material that have 4% visible light transmittance. The shade is lowered based on the amount of light falling on either the sensor (manual) or the window (automatic).

Conceptual dynamic shading: Daysim considers the operation of an idealized blind that covers all windows in the scene without the need for modeling the device geometrically. The effect of this blind is to reflect all direct sunlight and allow only 25% of diffuse sunlight into the space.

The control of dynamic shading devices uses the Lightswitch algorithm (Reinhart, 2004). This predicts the occupant discomfort and determine whether an occupant will lower a shade or not (lowered when DGP>0.4). Otherwise, occupants decide whether or not to lower the conceptual shading system by the presence of direct sunlight at each time step in the annual simulation.

Detailed dynamic shading: *Electrochromic glass:* is used to control glazing which changes state from mostly transparent to mostly opaque by switching out material definitions for a specific glazing material. This is a switchable shading systems that uses electrochromic glass that transition from clear to 30% transmission to 2% transmission.

Detailed dynamic shading: *Mechanical system:* This simulation used two perforated screens one with a transparency to opaque ratio of 3:4 and the other with 1:7 to control dynamic geometric shading.

Based on the simulations, the optimized window cover is the conceptual dynamic shade and the manual roller shades, they both creates a uniform UDI across the office tables. The electrochromic glass and the automatic roller shade brings in over 3000 lux close to the window. The mechanical shade blocks all the harmful radiation which made the office darker towards the end.

These experiments were carried out to demonstrate the current capabilities of simulating the operation of shading devices, that could affect the lighting distribution and the resulting visual comfort. Automatic shades can adapt to the external environmental factors and lighting conditions unlike static shades which do not block glare at all times. Although the work in this thesis is limited to static shading devices, it is possible to extend the workflow to include dynamic shading devices in future.

CHAPTER 3
METHODOLOGY

Chapter3.1. METHODOLOGY FOR GENERATING PATTERNS:

The Mashrabiyas are made of many thin and long bands and sticks that are assembled togethers to create a window like structures. These sticks are called "Mangour". They are assembled without glue or nail to stop the shrinkage and expansion caused by the weather. There are two types of Mangours, one made with a lathe, which results turneries and the other is made using a jigsaw with of solid pieces of wood and the result is flat shaped sticks. Both have the same concept but diverse ways of production (Figure 40).

Turneries
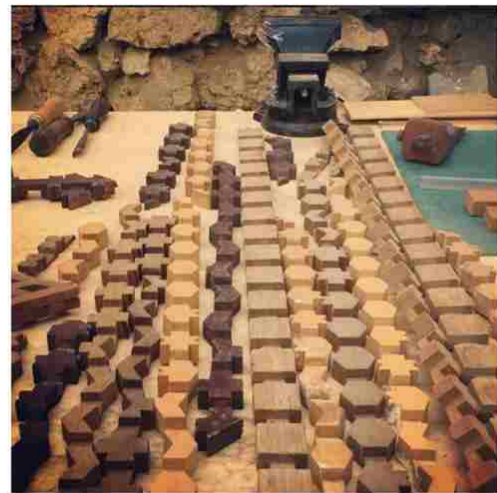
Mangours

Figure 40: Different types of manufacturing screens

Factors behind making them with sticks rather than one piece of wood, is the cost of wood, easy adjustment to fit any windows "just trim the long parts" and to ensure strength and sustainability of the piece.
There are three variables that must be taken into consideration during the making of each screen.
The pattern itself, the material used which is dependent on what was available (wood, stone, concrete,..etc.), and the way these patterns are embellished. To investigate these variables, line drawings must be analyzed.

Line Drawings:

Craftsmen were not mathematicians. They were skilled carvers and artists. The screens were calculated in length, width, and height to start a base grid, then they flourish with their beautiful designs using just a compass and a ruler. The most basic grid is the square grid and any pattern can be tessellated into a bigger composition. Furthermore, the same pattern can produce different tessellations, when rotated (Figure 41). Below are two examples of the same grid and pattern that appeared differently once rotated. The color coded image is for detecting the patterns in rotation. However interesting geometries are born at the intersection of each square.
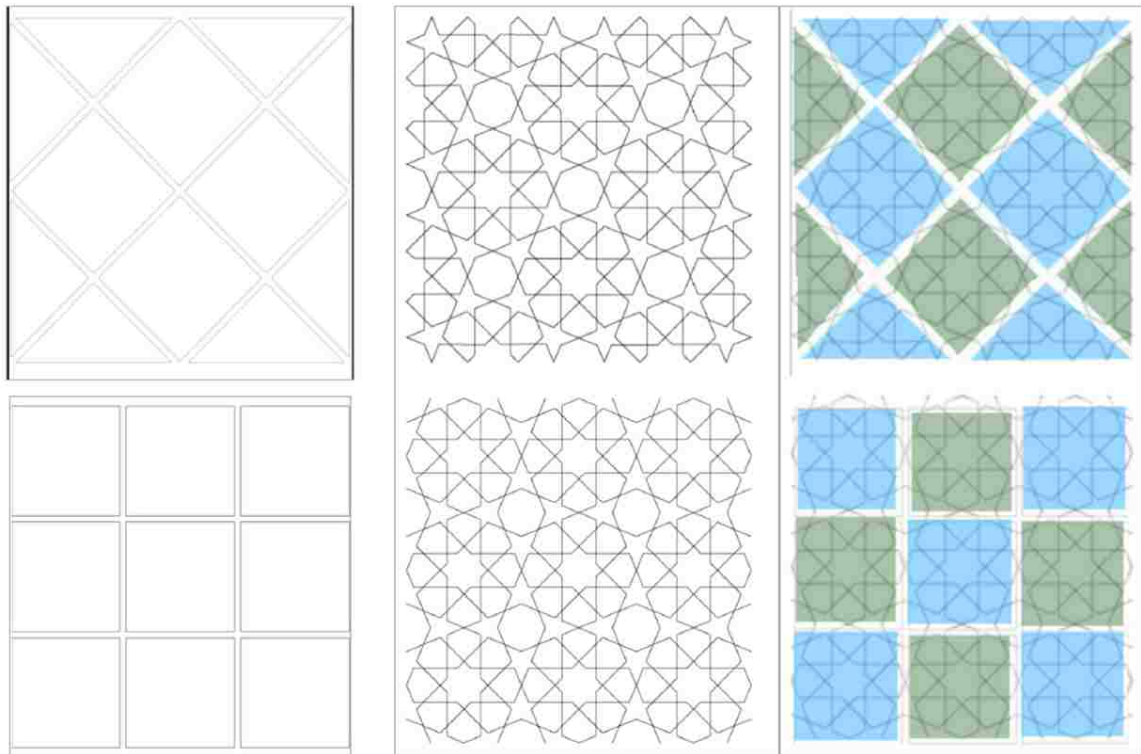
Figure 41: Results of the same patterns using rotated grids.

The visibility of the grid at the grand entrance of Sultan Al-Hassan Mosque in Egypt, Cairo (Figure 42) gave a way a trade secret. A similar example can be found in Bin Youssef Madrasa in Marrakech (Figure 43), where the grid is also visible on a plaster wall. The space is also known for its unusual star pattern at the entrance.

| Mosque Entrance | Pattern | Grid | Niche |
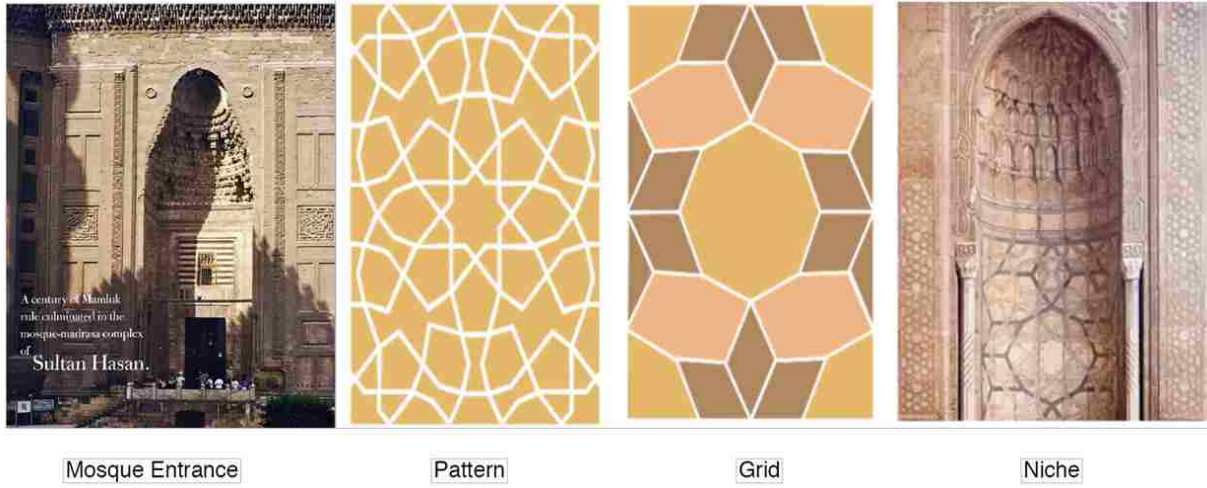
Figure 42: Sultan Hassan Mosque, Cairo, Egypt.
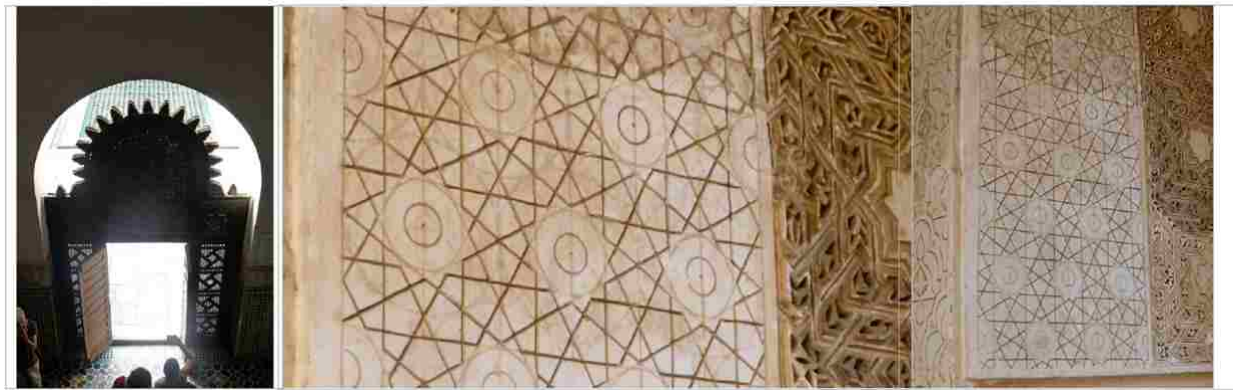
Figure 43: Bin Youssef Madrasa in Marrakech, Morocco

3.2 PARAMETRIZING ISLAMIC GEOMETRIES:

For simplicity, a square grid was chosen to create the patterns. Using visual programming language (Rhino Grasshopper), five definitions were created to generate these patterns. The result of weaving and trimming curves together presented computational challenges. Both generation of the patterns and their evaluation take enormous computational resources, which make them infeasible to model and analyze.
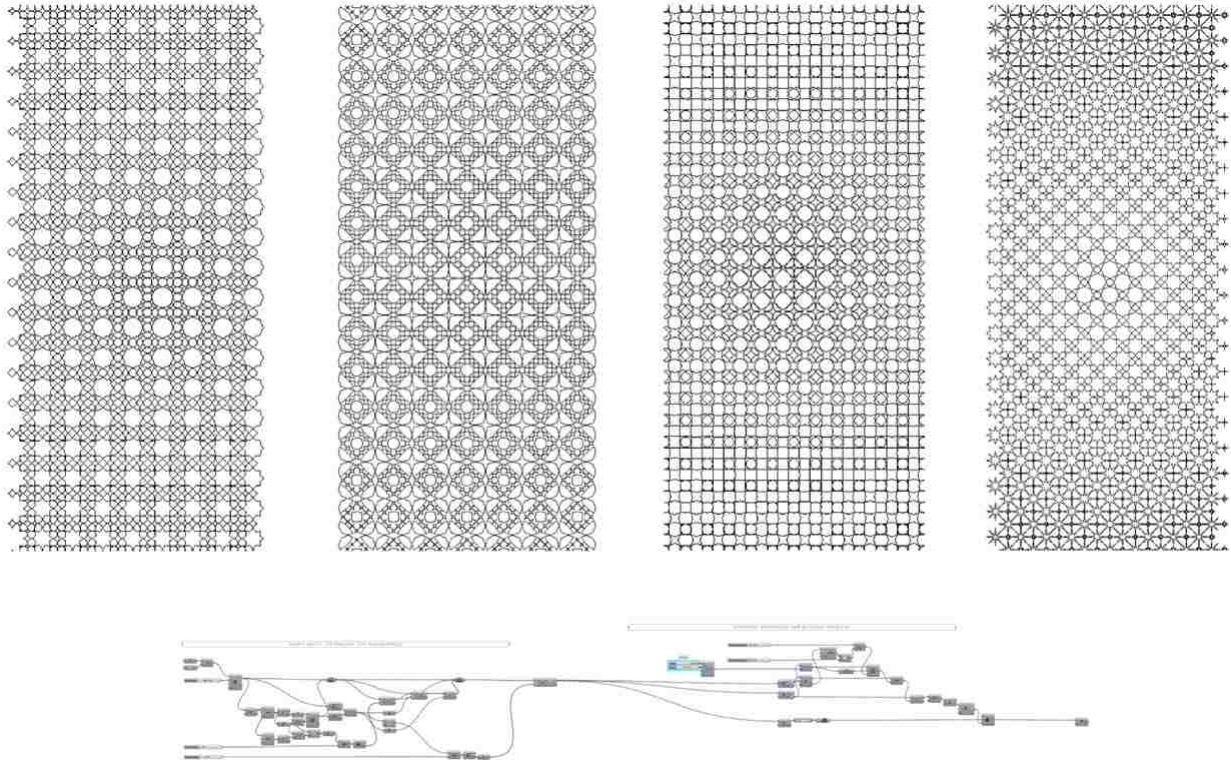
Figure 44: Visual programming language to develop definition for generating endless patterns.

These challenges were addressed by studying each created pattern. Each pattern consists of repeated modules that would generate a whole screen. To be able to successfully repeat each module, trial and error approach can be employed to finally get the desired screen (Figure 45). This could be a time consuming task.
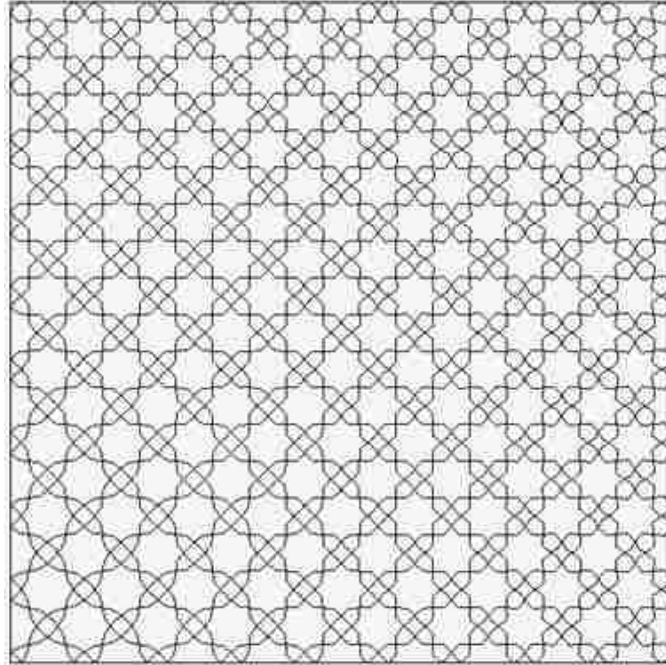
Figure 45: The target pattern

A better way would be to develop a systematic workflow, which can be achieved through implementing module extraction strategies. These strategies include:

    1.Finding the smallest module that could be repeated (Figure 46)

    2.The repetition must generate joined curves
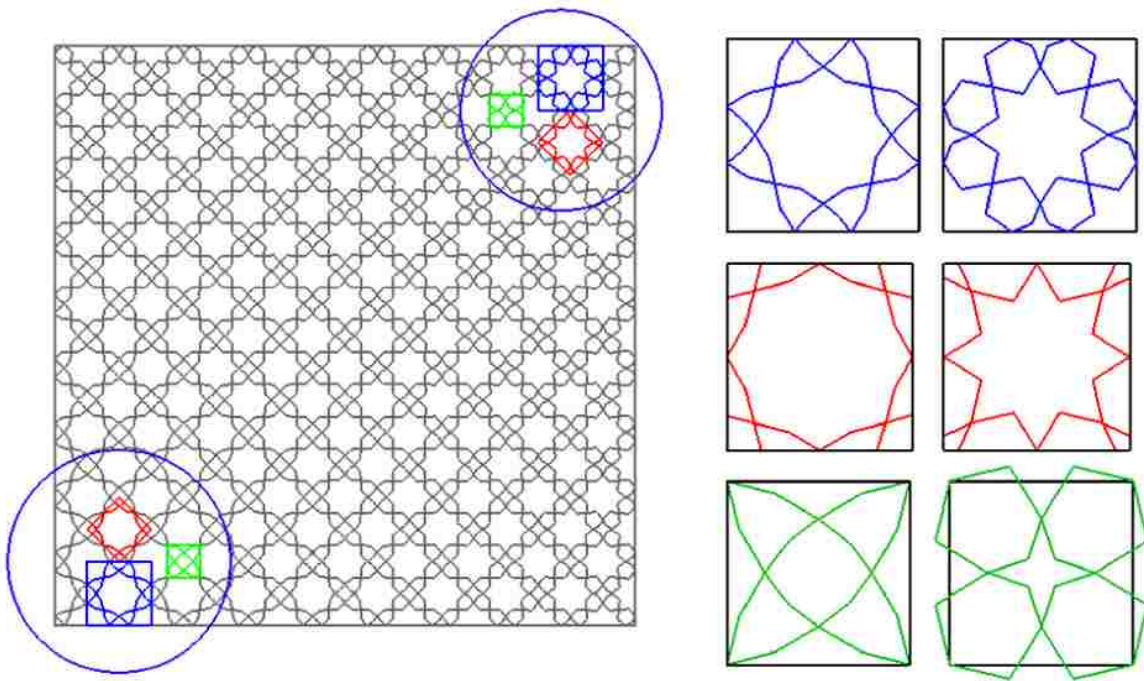
Figure 46: First strategy: Finding the smallest modules that could be repeated

After finding the smallest modules that could be repeated, testing them is required to find which module would generate closed curves and similar results to the target pattern. For example, the green module alternates and shifts in each row of the pattern. One grid would not generate the target pattern (Figure 47). In this case two grids are needed and the second grid must shift by 1 unit in order to reach the target pattern (Figure 48).
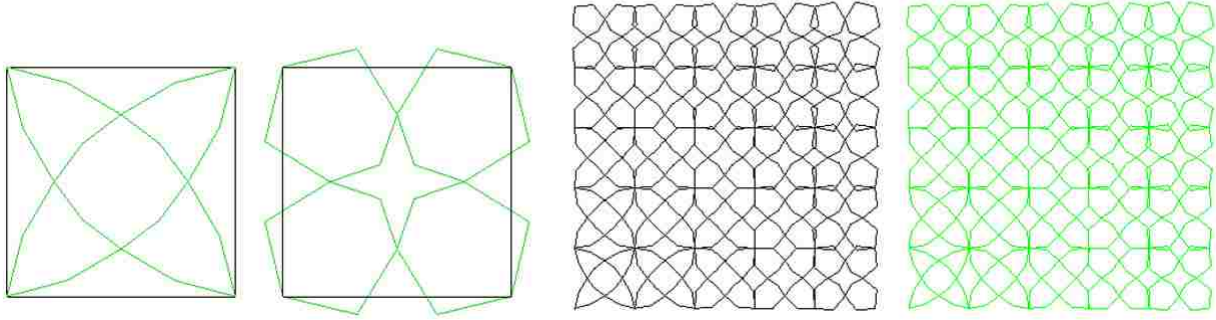
Figure 47: Second Strategy: Testing green modules with one grid
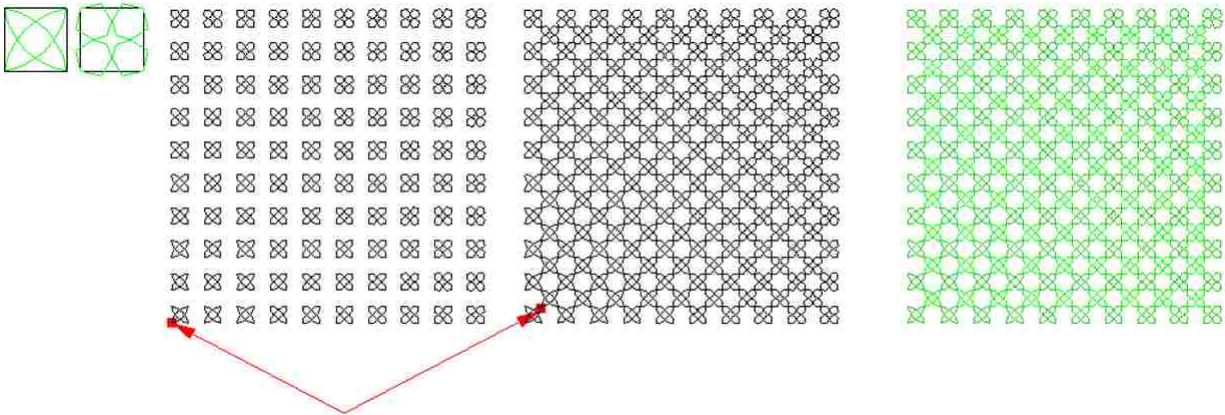
Figure 48: Second Strategy: Testing green modules with two grids.

If we follow the same strategies on the red pattern (Figure 49), different results emerge. The pattern looks similar to the target pattern, however it would not weave at its intersection (Figure 50).
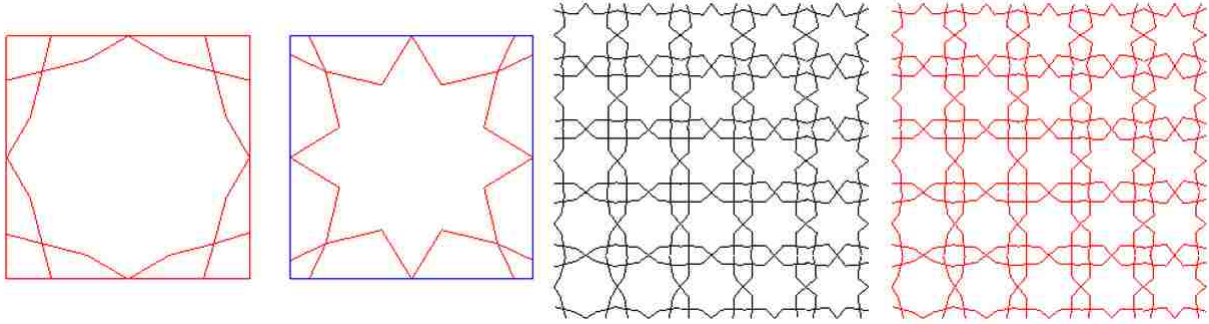
Figure 49: Second Strategy: Testing red modules.
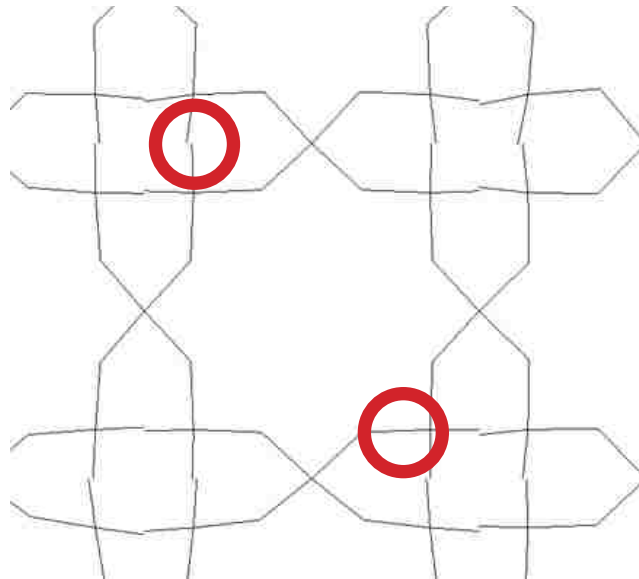
Figure 50: Second Strategy: Testing red modules points do not weave at intersections.

The third and final module is a more successful example. Only one grid is used and results a properly joined and weaved pattern.
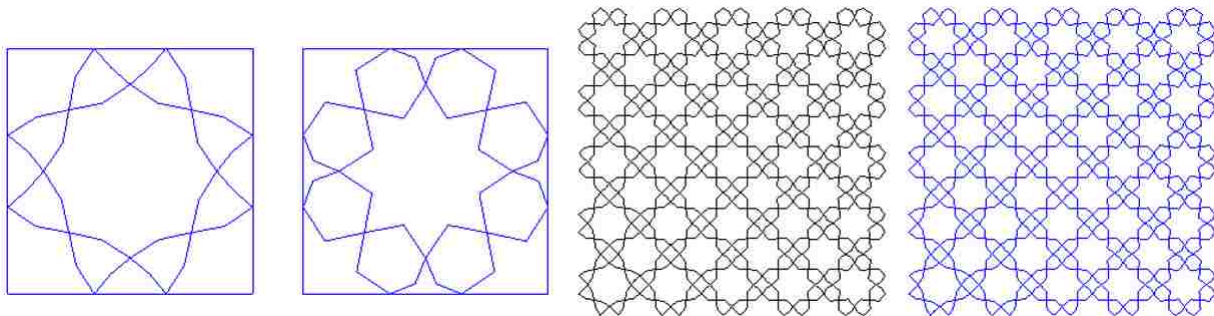
After choosing the best set of modules, a start and end pattern was chosen as an input for "custom 3D variable" – a Paneling tools component developed by Rajaa Issa for Grasshopper-. The component generates a list of tweened modules that can be extracted and analyzed for performance.

The result of this method (Figure 51) produced 2 sets of patterns, each has 17 modules with a 5% increment of openness factor in between (Figure 52). The efficiency of this pattern generation technique enables us to subject the patterns for advanced analysis.
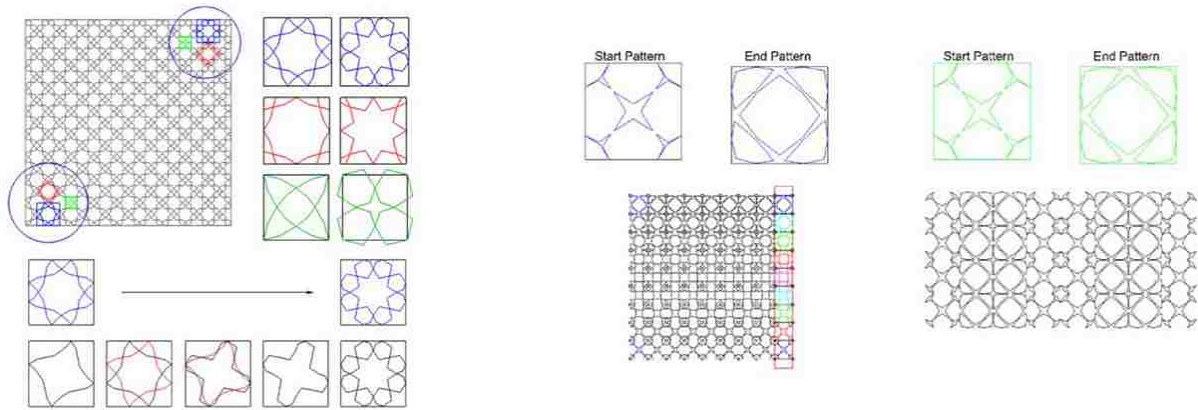
Figure 51: Creation of set 1 (Left), Creation of set 2 (right)
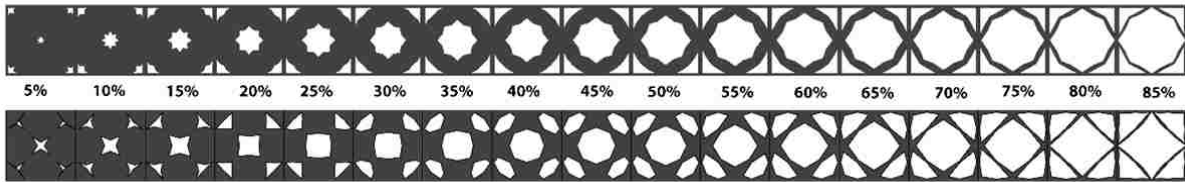
Figure 52: Set 1 (Top), Set 2 (Bottom), Total of 17 patterns in each set with 5% increments in between.

Chapter3.3. METHODOLOGY FOR EVALUATING PATTERNS:

Setting:

To gain insights on the performance of each module, a study model (Figure 53) with a south facing window was created in Rhino and grasshopper. The openness factor for the window is 95%, the model dimensions are 6x3.33x2.9 (DxWxH).
The unshaded window provides the base case, but screen with different patterns was employed to cover the window for further explorations. The screen was divided into a 20x20 grid. Each screen has 400 cells of the same pattern (Figure 54).
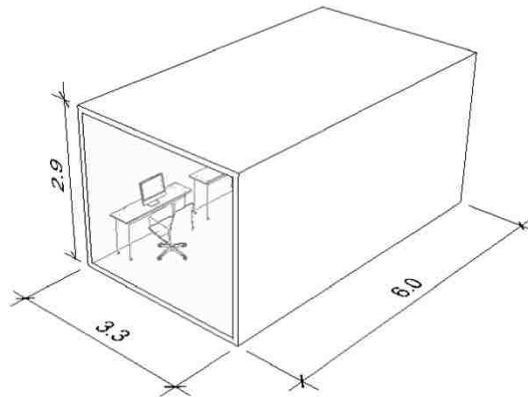
Figure 53: Base Case
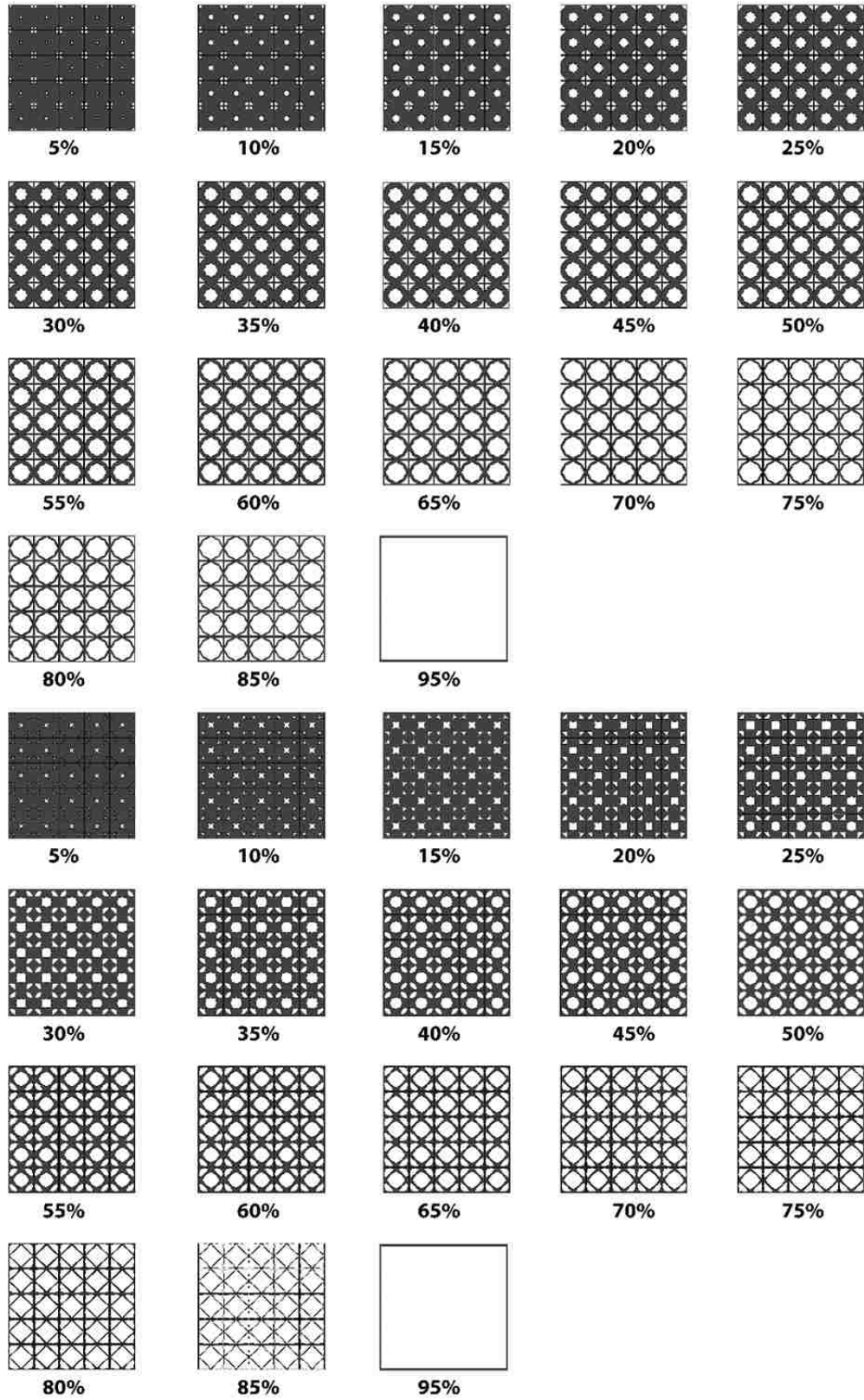
Figure 54: Partial elevation of the screen

3.4 EVALUATION CRITERIA:

For daylight simulations, the following metrics were analyzed (Figure 55) (Table 2):

Metric	Description of Metric	Description of Simulation	
DGP	The percentage of people disturbed by glare.	June, September, December 21 @ 12:00pm Clear Sky with sun Legend: >30 is considered glare.	Simulate 1st,2nd,3rd Desk
Vertical UDI	"Useful daylight illuminance" desired range on vertical surfaces	2m,4m,6m away from the window	1.1m, 2.2m ,3.3m away from East wall
<300 >3000	Underlit percentage affective in conjunction with artificial lighting Overlit percentage which can cause glare and visual discomfort	The legend scale follows the standard criteria, which is half the illuminance of the task surface which is 150-1500 Lux.	
ASE	ASE calculates the percentage of floor area that receives at least 1000 lux for at least 250 occupied hours per year which can cause glare.	ASE 1000, 250 lux	
Task Surface UDI	"Useful daylight illuminance" desired range on horizontal surfaces	.8m offset from floor	
<300 >3000	Underlit percentage affective in conjunction with artificial lighting Overlit percentage which can cause glare and visual discomfort	Standard UDI legend for task surfaces between 300 - 3000 Lux.	
ASE	ASE calculates the percentage of floor area that receives at least 1000 lux for at least 250 occupied hours per year which can cause glare.	ASE 1000, 250 lux	

Table2 : Initial simulation criteria and description of the metric used.
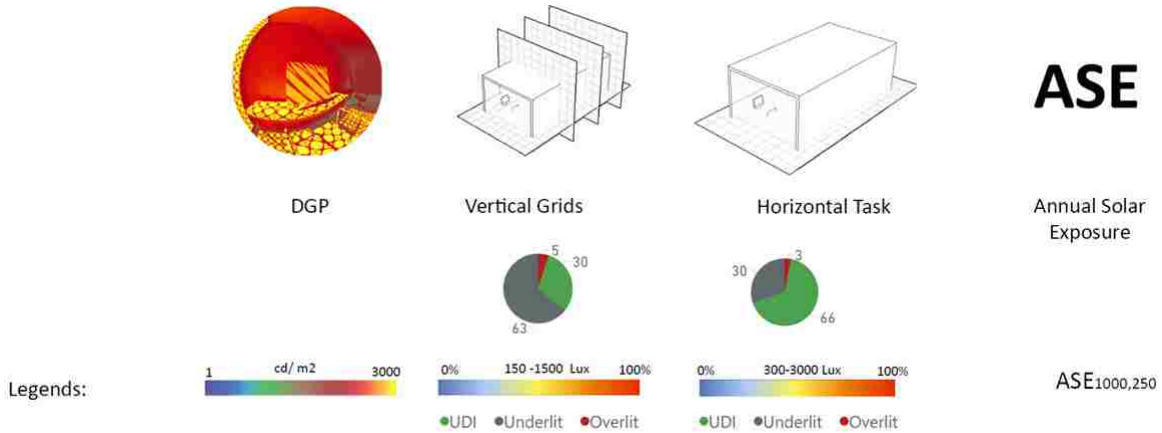
Figure 55: Initial simulation criteria

To be able to understand how sun penetration affect the space, multiple grids were located dividing the space into a waffle like vertical grids, placed either parallel to the window or facing it. Perpendicular grids are located on the east and west walls and they are also offset 1.1m away, which results in 4 grids. The grids parallel to the window were every 2m away from the window (Figure 57). A horizontal grid is created across the room at desk height.
The legends for vertical grids follow the standard practice, which is half the illuminance of the horizontal grids (DiLaura, 2011).

Glare was analyzed for this space, with and without furniture, for the first, second and the last desks (Figure 56).
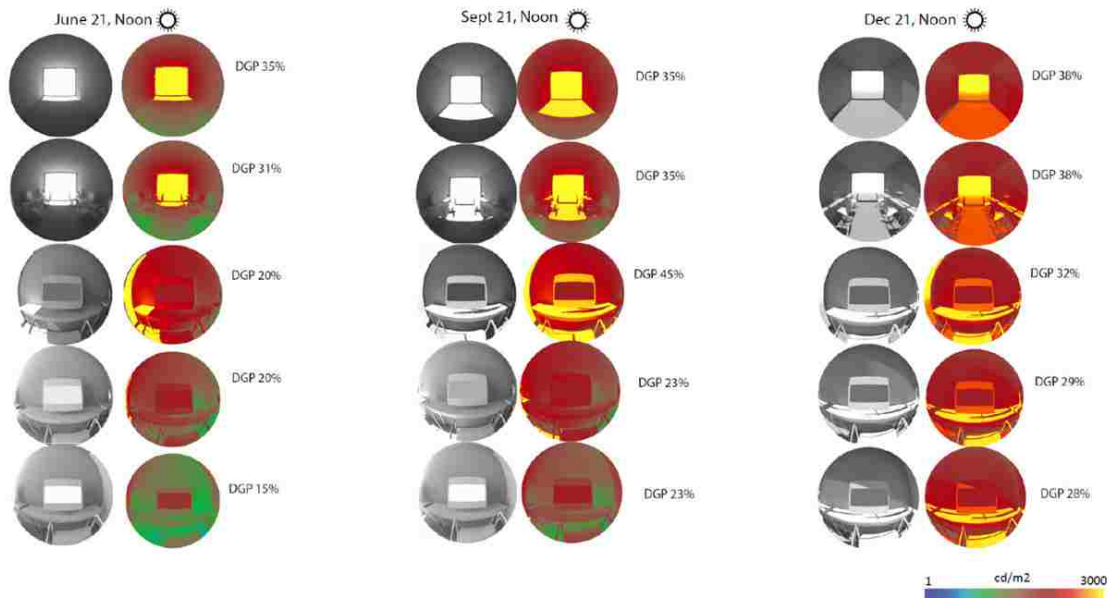
Figure 56: DGP analysis for the model with and without furniture, 1st, 2nd, and 3rd desks.
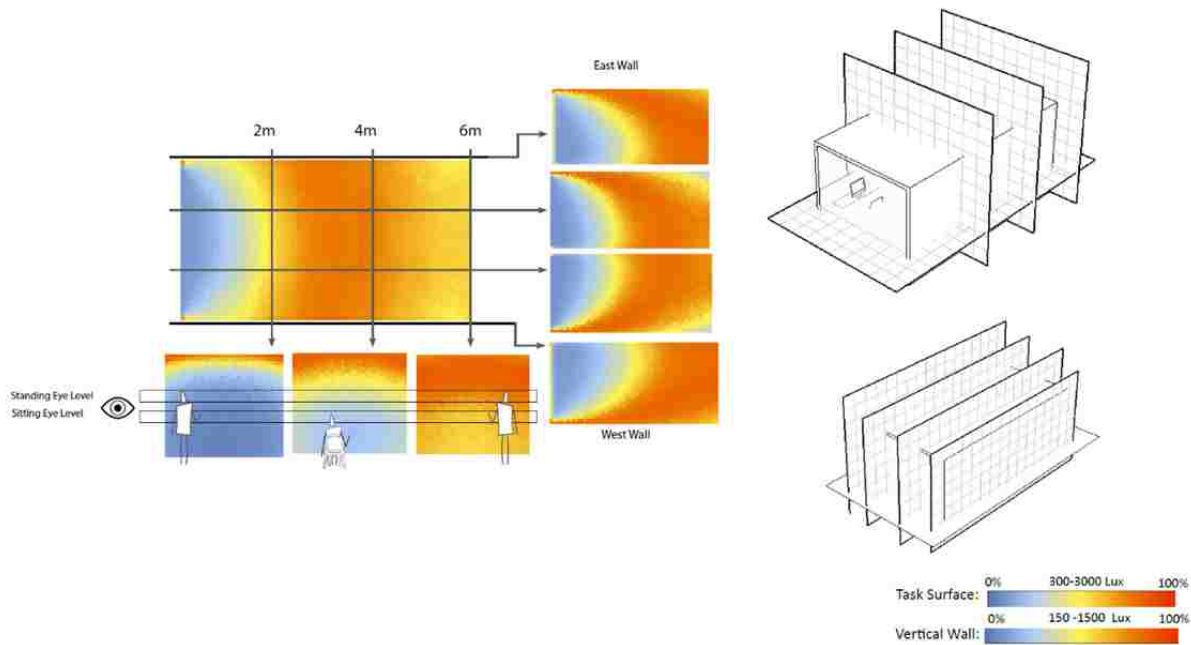
Figure 57: Daylight glare probability for the base case

Figure 57 demonstrates 7 vertical grids along with the horizontal grid. Given the extensiveness of the data and the time taken to generate the images, it is necessary to evaluate whether it is possible to reduce the number of simulations in the workflow. To eliminate the repeated or similar information that could be drawn from these 8 simulations, best differentiators to determine the effect of each screen on a designated space were identified as the 4m vertical grid away from the window, the task surface, and the DGP of the first deskthe The horizontal and vertical grids were analyzed using ASE, and UDA and the image of the first desk was evaluated using DGP (Figure58) (Table 3).

| Metric	Description of Metric	Description of Simulation	
DGP	The percentage of people disturbed by glare.	September21 @ 12:00pm Clear Sky with sun Legend: >30 is considered glare.	Simulate 1st Desk
Vertical UDI	"Useful daylight illuminance" desired range on vertical surfaces	2m away from the window	
<300	Underlit percentage affective in conjunction with artificial lighting	The legend scale follows the standard criteria, which is half the illuminance of the task surface which is 150-1500 Lux.	
>3000	Overlit percentage which can cause glare and visual discomfort		
ASE	ASE calculates the percentage of floor area that receives at least 1000 lux for at least 250 occupied hours per year which can cause glare.	ASE 1000, 250 lux	
Task Surface UDI	"Useful daylight illuminance" desired range on horizontal surfaces	.8m offset from floor	
<300	Underlit percentage affective in conjunction with artificial lighting	Standard UDI legend for task surfaces between 300 - 3000 Lux.	
>3000	Overlit percentage which can cause glare and visual discomfort		
ASE	ASE calculates the percentage of floor area that receives at least 1000 lux for at least 250 occupied hours per year which can cause glare.	ASE 1000, 250 lux	

Table 3 : Final simulation criteria and description of the metric used.


DGP
Sept 21, noon

Vertical Grids
at 2m

Horizontal Task

ASE

Annual Solar
Exposure

1   cd/m2   3000

0%   150 -1500 Lux   100%

0%   300-3000 Lux   100%

ASE 1000,250

●UDI ●Underlit ●Overlit

●UDI ●Underlit ●Overlit
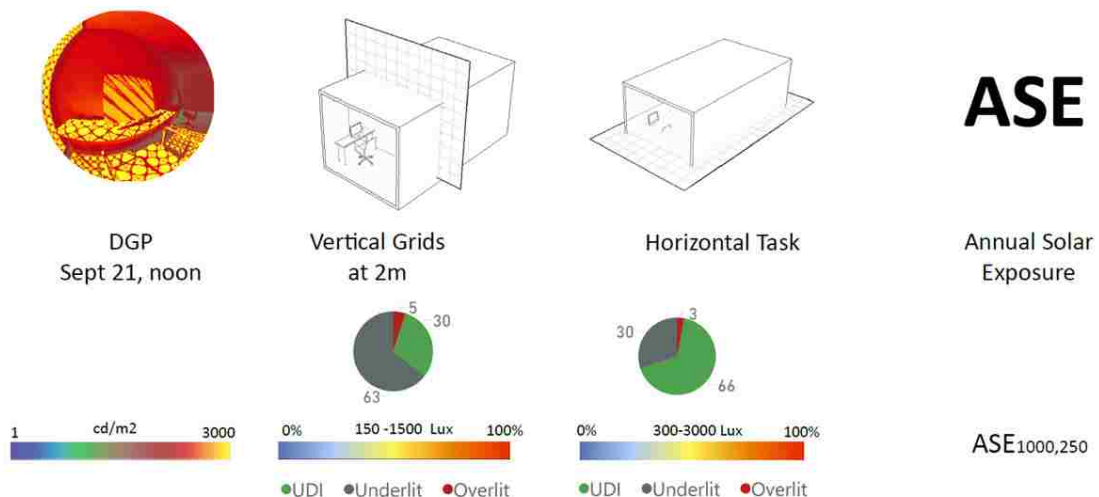
3.5 RADIANCE SETTINGS:

Each screen has 400 cells of the same pattern, which can result in expensive and time consuming simulations, a test of various parameters were studied.

Figure 59 presents the difference in simulations for default low and medium parameters for 5% and 50% openness factor. The difference in DGP results is not critical. However medium setting showed more accuracy in different openness factors.

The Radiance parameters for UDI settings have a significant effect on the simulation time, however the results in UDI on high and medium settings do not have significant differences.

The openness factor also impacts the simulation time. The tighter the pattern the more time it needs to simulate. For that reason, medium settings were chosen.

50% Open	50% Open	5% Open	5% Open
Radiance parameters:	Radiance parameters:	Radiance parameters:	Radiance parameters:
Low	medium	Low	medium
-ab 2	-ab 3	-ab 2	-ab 3
-aa .25	-aa .2	-aa .25	-aa .2
-ar 128	-ar 256	-ar 128	-ar 256
-ad 1028	-ad 2048	-ad 1028	-ad 2048
Time: 1 minutes	Time: 3 hours	Time: 10 minutes	Time: 5 hours
DGP: 34%	DGP: 35%	DGP: 5%	DGP: 5%
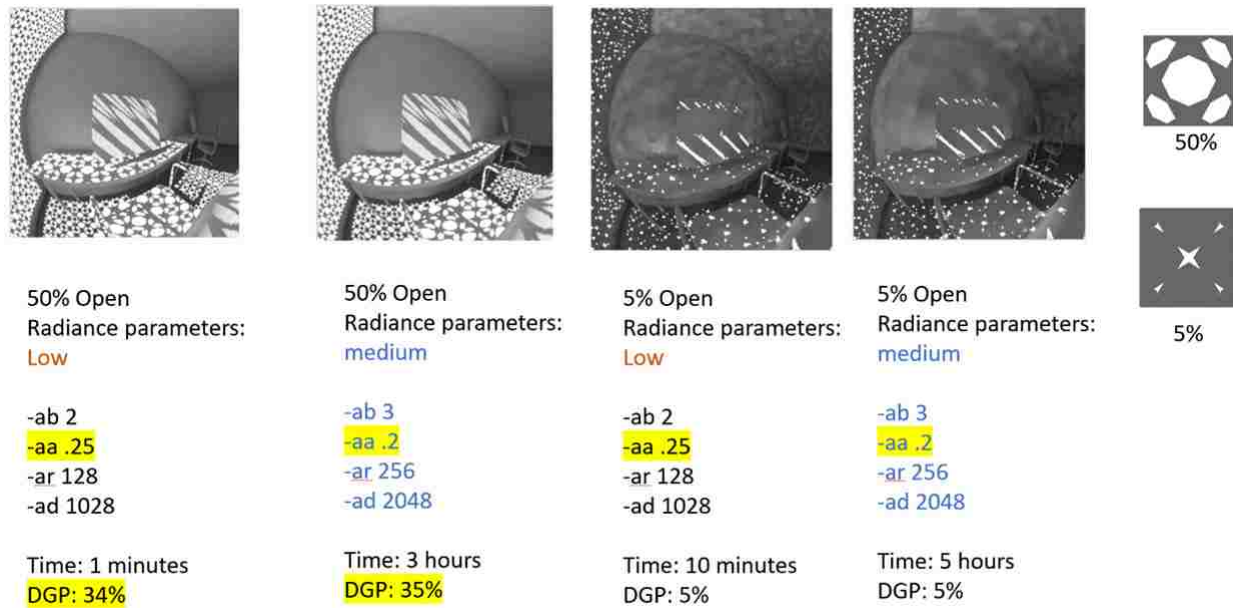
Figure 59: The effect of low and medium settings on different openness factors.
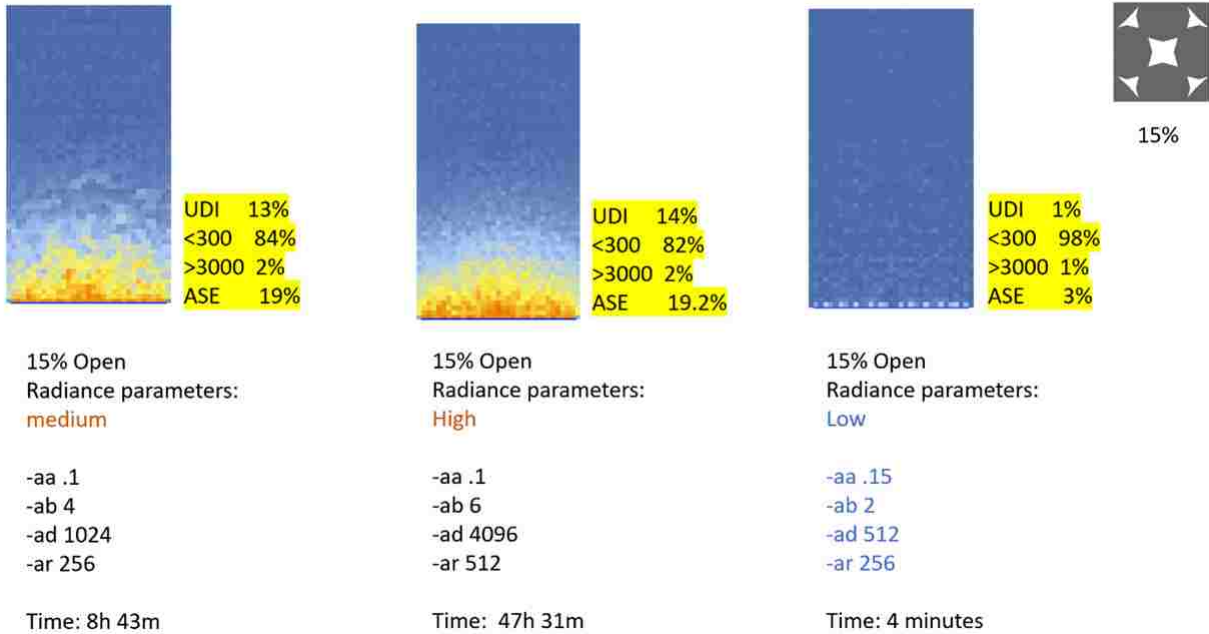
Figure 60: The effect of low, medium and high settings for 15% openness factors on simulation time and resolution.

CHAPTER 4
RESULTS

After running all simulations and comparing the results, it is clearly seen that the two patterns that have the same openness factor have identical results (Figure 61,62) (Table 4,5) This is a significant finding. This means that the design of the pattern doesn't drive the performance of the space and the openness factor have a huge impact on the performance. Or to put it in other words, the user can choose any design they would prefer, and the openness factor should be decided based on the desired performance outcome. Even further, it negates the need to repeat the simulations over and over to choose a particular pattern.

To illustrate this point, a random pattern with the same openness factor was simulated, and the results were identical (Figure 63).

To illustrate the results of the simulation with 60% openness factor of a random pattern was performed.

The simulation results match the conclusion.

Figure 61: Results for set1 pattern simulation
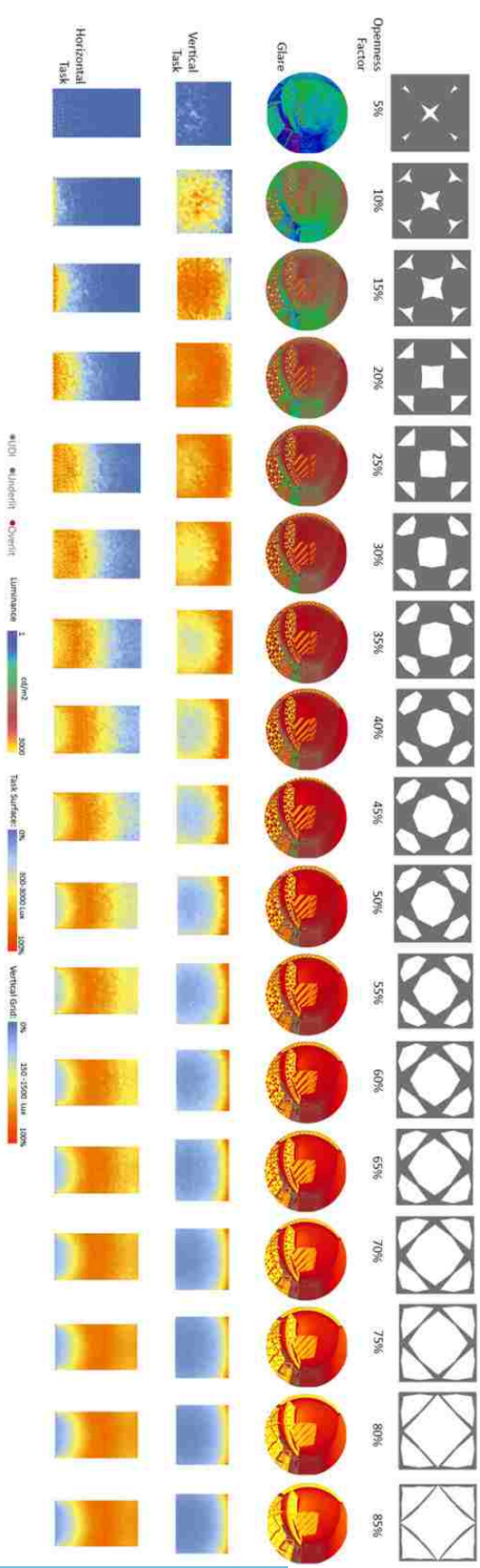
Figure 62: Results for set2 pattern simulation

Set 1

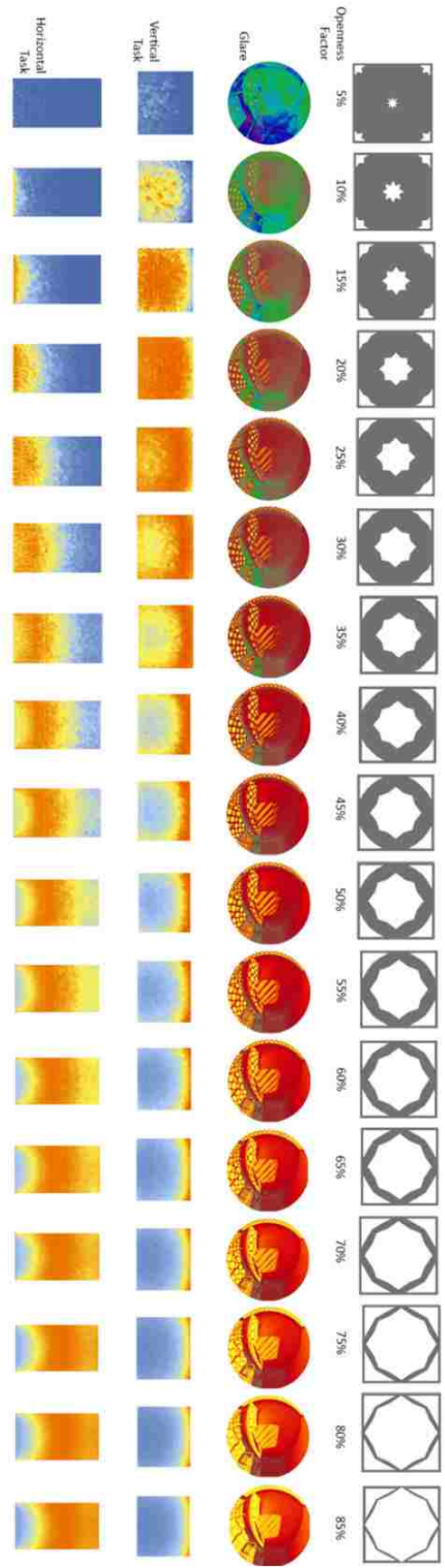| Pattern Image																	
Openness Factor	5%	10%	15%	20%	25%	30%	35%	40%	45%	50%	55%	60%	65%	70%	75%	80%	85%
DGP	8%	26%	26%	25%	27%	28%	30%	31%	33%	35%	36%	38%	40%	40%	42%	44%	46%
UDI V	4%	37%	66%	74%	72%	66%	59%	51%	44%	38%	33%	29%	26%	23%	21%	20%	19%
Underlit V	94%	61%	30%	18%	13%	11%	9%	7%	7%	6%	6%	5%	5%	5%	5%	4%	4%
Overlit V	1%	2%	3%	7%	14%	22%	31%	40%	48%	55%	60%	65%	68%	70%	73%	74%	75%
ASE V	1%	5%	11%	19%	26%	34%	43%	50%	55%	59%	61%	63%	65%	66%	68%	70%	71%
UDI H	1%	5%	13%	22%	30%	38%	44%	49%	53%	56%	58%	60%	61%	61%	61%	61%	61%
Underlit H	98%	92%	83%	73%	63%	55%	47%	40%	34%	28%	25%	22%	19%	17%	15%	15%	14%
Overlit H	1%	1%	2%	3%	5%	6%	8%	10%	12%	14%	15%	17%	18%	20%	22%	23%	24%
ASE H	5%	12%	19%	25%	29%	32%	35%	38%	41%	44%	45%	46%	48%	49%	51%	52%	52%

Set 2

Pattern Image																	
Openness Factor	5%	10%	15%	20%	25%	30%	35%	40%	45%	50%	55%	60%	65%	70%	75%	80%	85%
DGP	5%	24%	25%	26%	27%	29%	30%	31%	33%	35%	36%	38%	40%	40%	42%	44%	45%
UDI V	2%	41%	66%	74%	72%	64%	59%	50%	43%	38%	33%	29%	26%	23%	21%	20%	19%
Underlit V	96%	56%	30%	17%	13%	10%	9%	7%	7%	6%	6%	5%	5%	5%	5%	4%	4%
Overlit V	1%	2%	3%	7%	14%	24%	32%	41%	48%	55%	60%	64%	68%	71%	73%	74%	75%
ASE V	2%	4%	11%	20%	30%	39%	44%	50%	55%	59%	62%	64%	67%	68%	69%	70%	71%
UDI H	1%	6%	13%	23%	31%	38%	43%	49%	53%	56%	58%	60%	61%	61%	61%	61%	61%
Underlit H	98%	92%	84%	72%	62%	54%	47%	40%	34%	29%	25%	22%	19%	17%	16%	15%	14%
Overlit H	1%	2%	2%	4%	5%	7%	8%	10%	12%	14%	15%	17%	19%	20%	22%	23%	24%
ASE H	3%	14%	19%	26%	31%	35%	37%	39%	41%	43%	45%	47%	48%	49%	50%	51%	52%

Table 4-5: Simulation results for set1 and set 2.
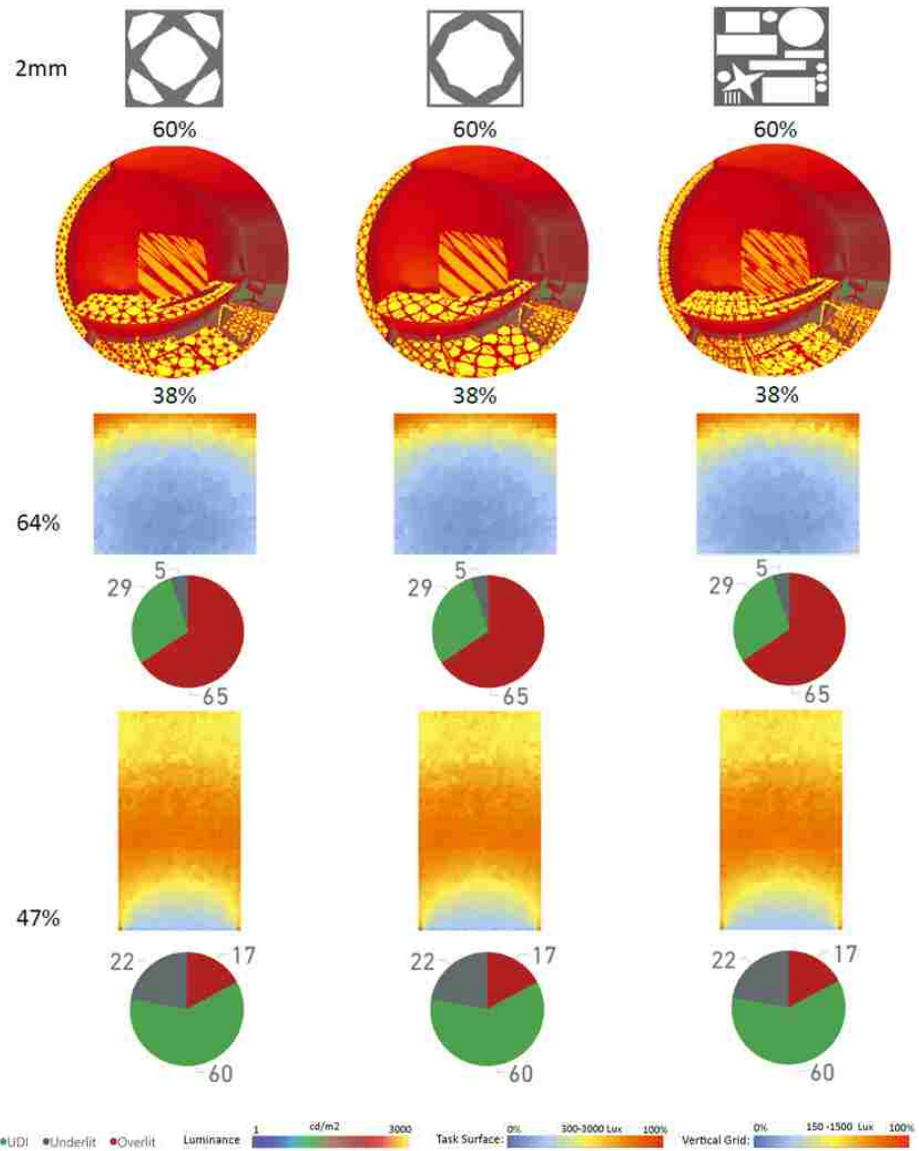
Figure 63: Identical results for a random pattern with 60% openness factor.
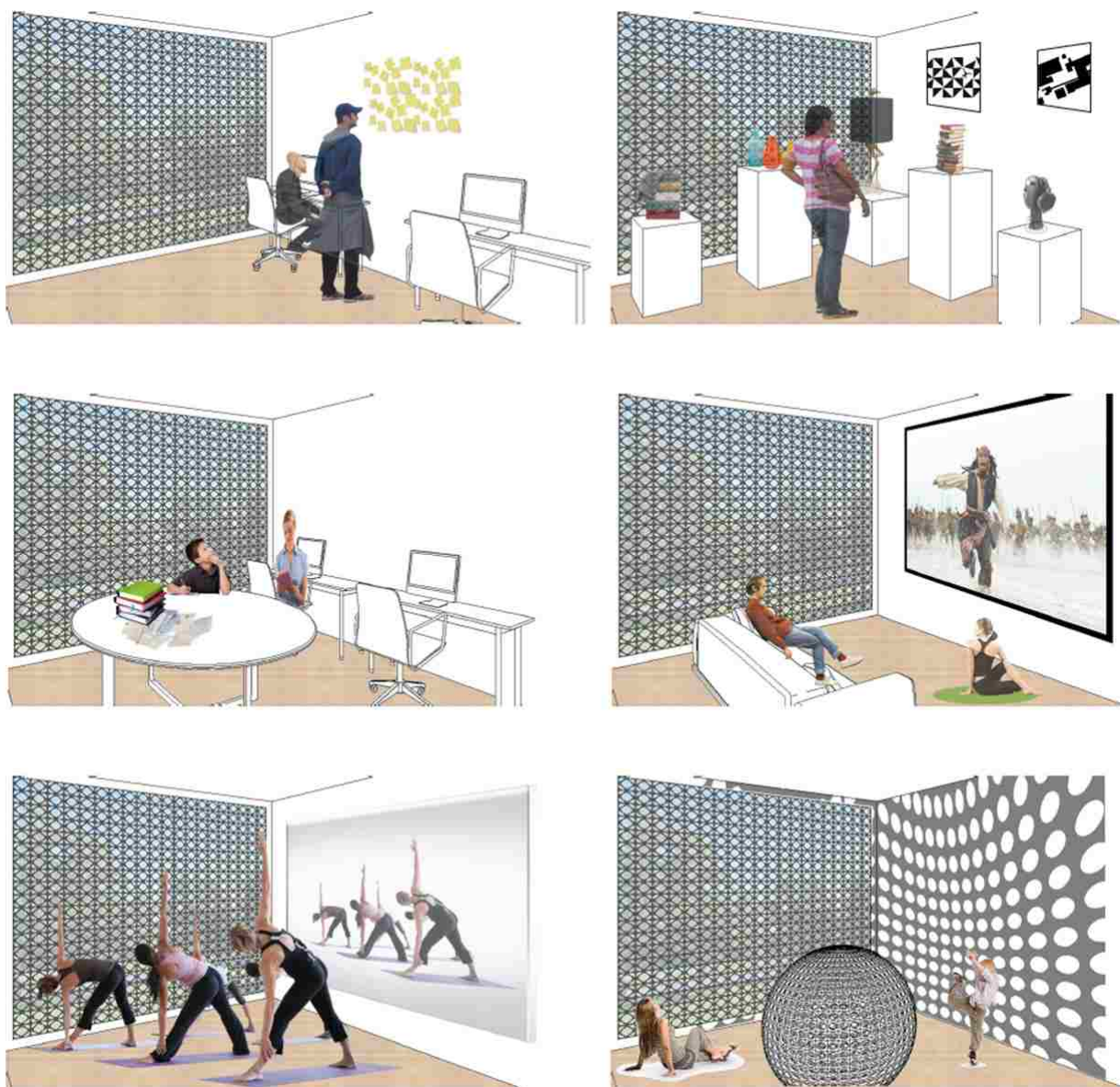
Figure 64: Evaluation of screens based on different functionality of the space.

We have established that the design of the pattern doesn't drive the results. Then the focus is the openness factor and how it would affect the performance of a room. The desired openness depends on the intended luminous environment. The following criteria are identified to study the wide ranging luminous environments:

1. Light control for common visual tasks
2. Light control for vertical tasks
3. Light control for horizontal tasks
4. Light control for Dim environments
5. Diffuse environments
6. Environments that are designed for the presence and animation of solar beams

1. Light control for common visual tasks:

Spaces such as offices and libraries incorporate both horizontal and vertical task surfaces. Therefore, this group of spaces would benefit from studying both horizontal and vertical grids and DGP.

Looking back at figure 61, none of the openness factors match the criteria needed for lighting control of both horizontal and vertical visual tasks.
The best performing pattern has a 40% openness factor. The reasoning behind the selection is that 40% provides 50% useful lighting in both vertical and horizontal tasks (Table 6). However, both DGP and ASE results are very high. The overall evaluation is that the openness factor alone does not yield satisfying solutions, and other factors such as the thickness of the shade must be taken into consideration for further development (Figure 64).

Light Control for Common Visual Tasks:

DGP	≤ 30%

Vertical Grid:

UDI	>70%
Underlit	<15%
Overlit	<15%
ASE	<15%

Task Surface:

UDI	>70%
Underlit	<15%
Overlit	<15%
ASE	<15%

Pattern Image																	
Openness Factor	5%	10%	15%	20%	25%	30%	35%	40%	45%	50%	55%	60%	65%	70%	75%	80%	85%
DGP	5%	24%	25%	26%	27%	29%	30%	31%	33%	35%	36%	38%	40%	40%	42%	44%	45%
UDI V	2%	41%	66%	74%	72%	64%	59%	50%	43%	38%	33%	29%	26%	23%	21%	20%	19%
Underlit V	96%	56%	30%	17%	13%	10%	9%	7%	7%	6%	6%	5%	5%	5%	5%	4%	4%
Overlit V	1%	2%	3%	7%	14%	24%	32%	41%	48%	55%	60%	64%	68%	71%	73%	74%	75%
ASE V	2%	4%	11%	20%	30%	39%	44%	50%	55%	59%	62%	64%	67%	68%	69%	70%	71%
UDI H	1%	8%	13%	23%	31%	38%	43%	49%	53%	56%	58%	60%	61%	61%	61%	61%	61%
Underlit H	98%	92%	84%	72%	62%	54%	47%	40%	34%	29%	25%	22%	19%	17%	16%	15%	14%
Overlit H	1%	2%	3%	4%	5%	7%	8%	10%	12%	14%	15%	17%	19%	20%	22%	23%	24%
ASE H	3%	14%	19%	26%	31%	35%	37%	39%	41%	43%	45%	47%	48%	49%	50%	51%	52%

Table 6: Highlights the most ideal openness factor for common visual tasks.
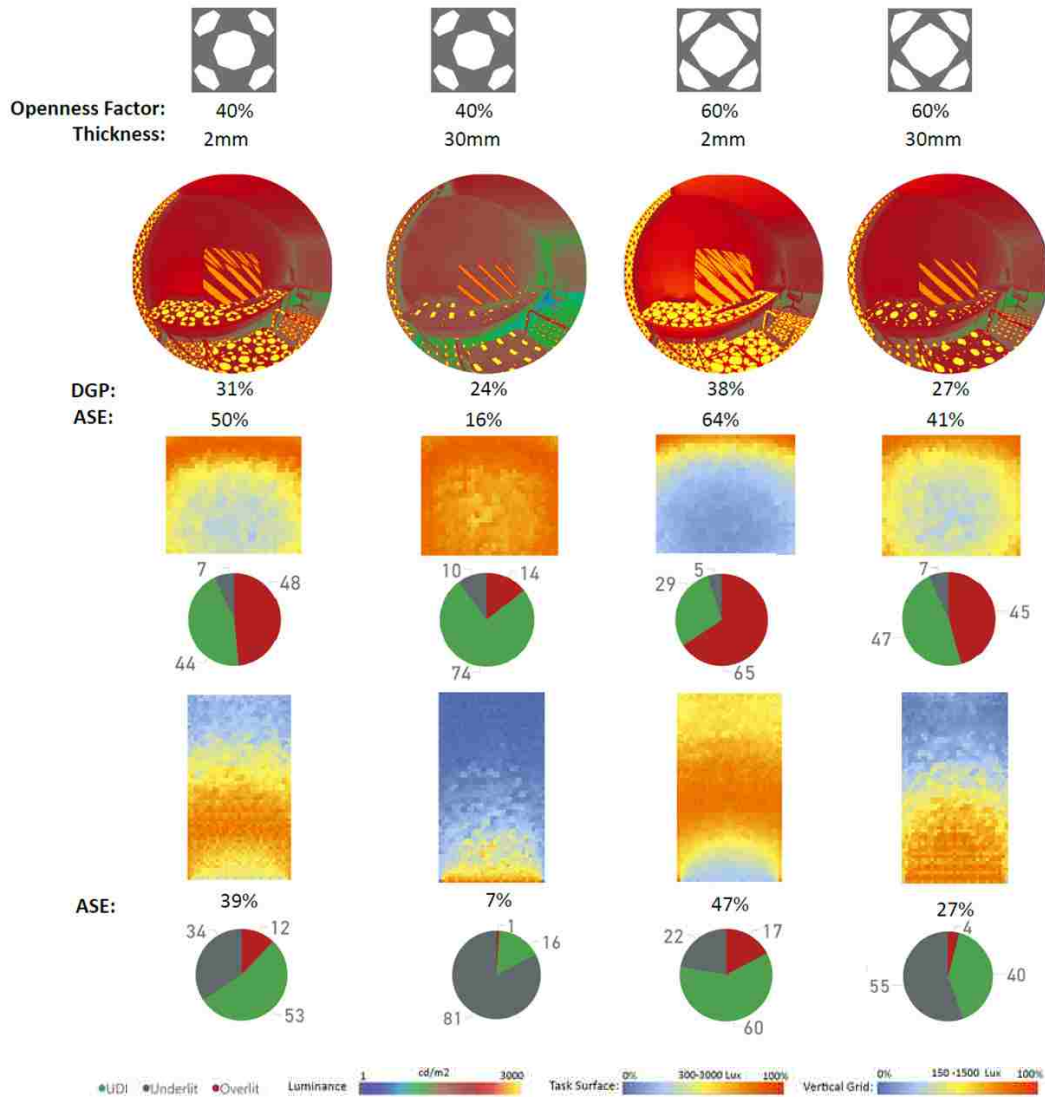
Figure 65: Comparing screens for common visual tasks with different thicknesses.

A 40% openness factor with 2mm thickness provides 50% UDI on both Vertical and Horizontal tasks, but when thickness is increased to 30mm, glare drops from 31% to 24%, UDI vertical increases, and UDI horizontal decrease.

In this particular case, higher openness factor is required to maintain the performance of the space. Therefore, selection of a screen becomes more meaningful if the openness factor and thickness are concurrently parametrized.

2. Light control for common Vertical tasks:

Examples: Store, Wall Décor, Computer screens. The main task is considered to be the vertical surface, and results from vertical grids guide the design decisions along with DGP.
The previous simulations and analysis indicate that with a 2mm thickness, the openness factor from 20% to 25% is ideal for vertical tasks (Figure 61) (Table 7).

Light Control for Common Vertical Tasks:

DGP	≤ 30%

Vertical Grid:	
UDI	>70%
Underlit	<15%
Overlit	<15%
ASE	<15%

Pattern Image																	
Openness Factor	5%	10%	15%	20%	25%	30%	35%	40%	45%	50%	55%	60%	65%	70%	75%	80%	85%
DGP	5%	24%	25%	26%	27%	29%	30%	31%	33%	35%	36%	38%	40%	40%	42%	44%	45%
UDI V	2%	41%	66%	74%	72%	64%	59%	50%	43%	38%	33%	29%	26%	23%	21%	20%	19%
Underlit V	96%	58%	30%	17%	13%	10%	9%	7%	7%	8%	6%	5%	5%	5%	5%	4%	4%
Overlit V	1%	2%	3%	7%	14%	24%	32%	41%	48%	55%	60%	64%	68%	71%	73%	74%	75%
ASE V	2%	4%	11%	20%	30%	39%	44%	50%	55%	59%	62%	64%	67%	68%	69%	70%	71%
UDI H	1%	6%	13%	23%	31%	38%	43%	49%	53%	56%	58%	60%	61%	61%	61%	61%	61%
Underlit H	98%	92%	84%	72%	62%	54%	47%	40%	34%	29%	25%	22%	19%	17%	16%	15%	14%
Overlit H	1%	2%	2%	4%	5%	7%	8%	10%	12%	14%	15%	17%	19%	20%	22%	23%	24%
ASE H	3%	14%	19%	26%	31%	35%	37%	39%	41%	43%	45%	47%	48%	49%	50%	51%	52%

Table 7: Ideal openness factor for vertical tasks.

3.Light control for common Horizontal tasks:

Example: School, Office, Library

Light Control for Common Horizontal Tasks:

DGP	≤ 30%

Vertical Grid:

UDI	>70%
Underlit	<15%
Overlit	<15%
ASE	<15%

Pattern Image																	
Openness Factor	5%	10%	15%	20%	25%	30%	35%	40%	45%	50%	55%	60%	65%	70%	75%	80%	85%
DGP	5%	24%	25%	26%	27%	29%	30%	31%	33%	35%	38%	38%	40%	40%	42%	44%	45%
UDI V	2%	41%	66%	74%	72%	64%	59%	50%	43%	38%	33%	29%	26%	23%	21%	20%	19%
Underlit V	96%	56%	30%	17%	13%	10%	9%	7%	7%	6%	8%	5%	5%	5%	5%	4%	4%
Overlit V	1%	2%	3%	7%	14%	24%	32%	41%	48%	55%	60%	64%	68%	71%	73%	74%	75%
ASE V	2%	4%	11%	20%	30%	39%	44%	50%	55%	59%	62%	64%	67%	68%	69%	70%	71%
UDI H	1%	6%	13%	23%	31%	38%	43%	49%	53%	56%	58%	60%	61%	61%	61%	61%	61%
Underlit H	98%	92%	84%	72%	62%	54%	47%	40%	34%	29%	25%	22%	19%	17%	16%	15%	14%
Overlit H	1%	2%	2%	4%	5%	7%	8%	10%	12%	14%	15%	17%	19%	20%	22%	23%	24%
ASE H	3%	14%	19%	26%	31%	35%	37%	39%	41%	43%	45%	47%	48%	49%	50%	51%	52%

Table 8: Ideal openness factor for horizontal tasks.

Similar to common visual tasks, there isn't an optimum solution for performance within these simulation results (Table 8). The wider the openness factor is the more glare and sun it presents. In this case, thickness is a solution for preventing glare and reducing sun exposure (figure 66).
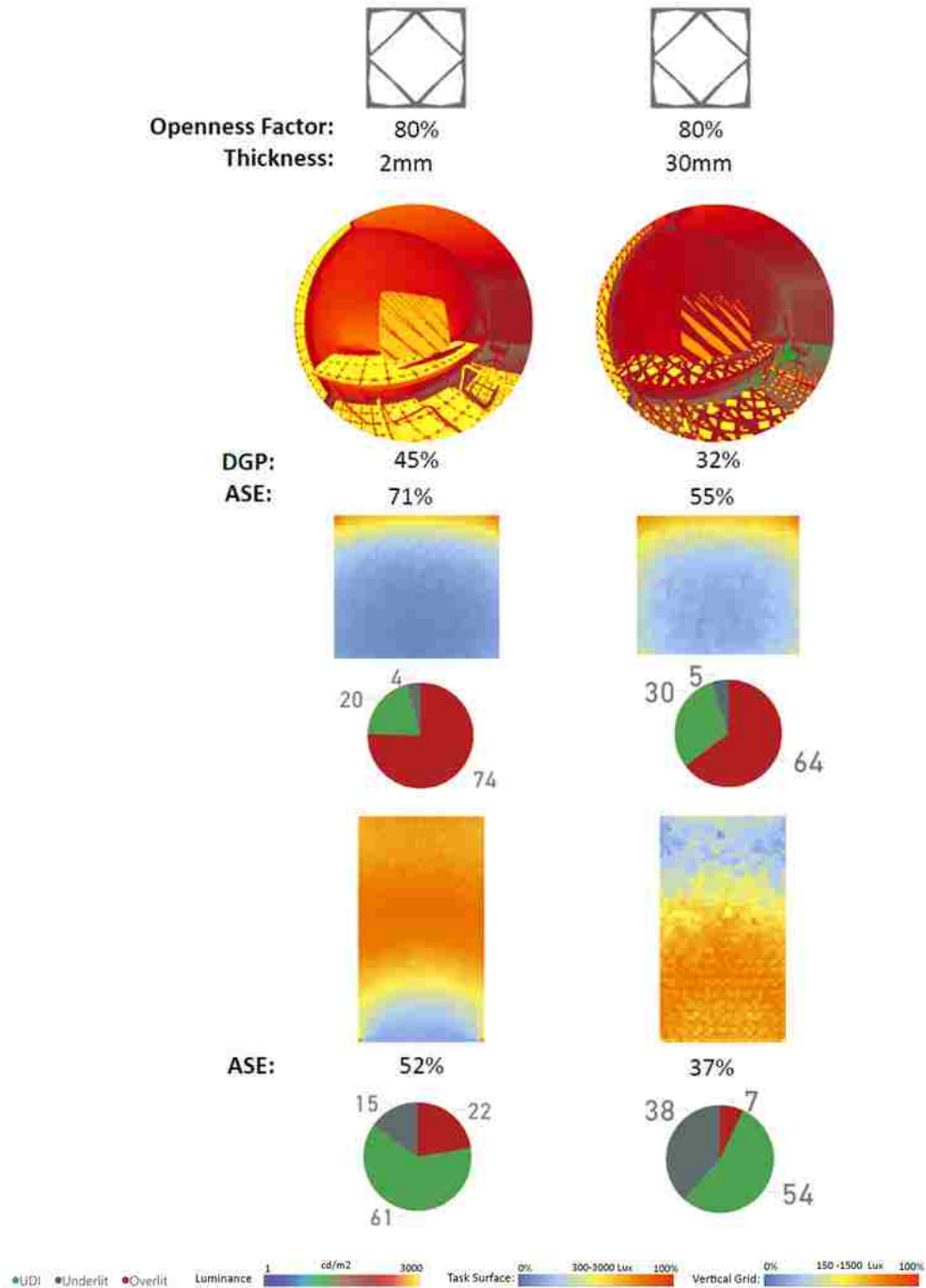
Figure 66: Thickness reduces glare, sun exposure and impoves the visual quality of the room.

When tested with 30% thickness, DGP was reduced by 13% , ASE and Overlit on the horizontal task surface was decreased by 15%.

4.Light control for Dim environments:

Example: Presentation rooms, Home Theater. For a dim environment, a smaller openness factor is needed depending on the lighting levels needed in the space.
If a wider openness factor is desired, then a thicker screen must be taken into consideration.

Light Control for Dim Environments:

DGP	≤ 30%

Vertical Grid:

UDI	<15%
Underlit	>70%
Overlit	<15%
ASE	<10%

Pattern Image																	
Openness Factor	5%	10%	15%	20%	25%	30%	35%	40%	45%	50%	55%	60%	65%	70%	75%	80%	85%
DGP	5%	24%	25%	26%	27%	29%	30%	31%	33%	35%	36%	38%	40%	40%	42%	44%	45%
UDI V	2%	41%	66%	74%	72%	64%	59%	50%	43%	38%	33%	29%	26%	23%	21%	20%	19%
Underlit V	96%	56%	30%	17%	13%	10%	9%	7%	7%	8%	8%	5%	5%	5%	5%	4%	4%
Overlit V	1%	2%	3%	7%	14%	24%	32%	41%	48%	55%	60%	64%	68%	71%	73%	74%	75%
ASE V	2%	4%	11%	20%	30%	39%	44%	50%	55%	59%	62%	84%	67%	68%	69%	70%	71%
UDI H	1%	6%	13%	23%	31%	38%	43%	49%	53%	56%	58%	60%	61%	61%	61%	61%	61%
Underlit H	98%	92%	84%	72%	62%	54%	47%	40%	34%	29%	25%	22%	19%	17%	16%	15%	14%
Overlit H	1%	2%	2%	4%	5%	7%	8%	10%	12%	14%	15%	17%	19%	20%	22%	23%	24%
ASE H	3%	14%	19%	26%	31%	35%	37%	39%	41%	43%	45%	47%	48%	49%	50%	51%	52%

Table 9: Light control for dim environments

Figure 66: The effect of thickness on a space with small openness factor.

5.Diffused Light:

Example: Gym, Musuem. For diffused light environment, ASE must be low. A smaller openness factor provides low ASE and a dark environment.
A thicker screen with a wide openness factor would reduce ASE and provide the space with diffused lighting.

Pattern Image																	
Openness Factor	5%	10%	15%	20%	25%	30%	35%	40%	45%	50%	55%	60%	65%	70%	75%	80%	85%
DGP	5%	24%	25%	26%	27%	29%	30%	31%	33%	35%	36%	38%	40%	40%	42%	44%	45%
UDI V	2%	41%	66%	74%	72%	64%	59%	50%	43%	38%	33%	29%	26%	23%	21%	20%	19%
Underlit V	96%	56%	30%	17%	13%	10%	9%	7%	7%	6%	6%	5%	5%	5%	5%	4%	4%
Overlit V	1%	2%	3%	7%	14%	24%	32%	41%	48%	55%	60%	64%	68%	71%	73%	74%	75%
ASE V	2%	4%	11%	20%	30%	39%	44%	50%	55%	59%	62%	64%	67%	68%	69%	70%	71%
UDI H	1%	6%	13%	23%	31%	38%	43%	49%	53%	56%	58%	60%	61%	61%	61%	61%	61%
Underlit H	98%	92%	84%	72%	62%	54%	47%	40%	34%	29%	25%	22%	19%	17%	16%	15%	14%
Overlit H	1%	2%	2%	4%	5%	7%	8%	10%	12%	14%	15%	17%	19%	20%	22%	23%	24%
ASE H	3%	14%	19%	26%	31%	35%	37%	39%	41%	43%	45%	47%	48%	49%	50%	51%	52%

Table 10: Choosing openness factor for a dim environment.
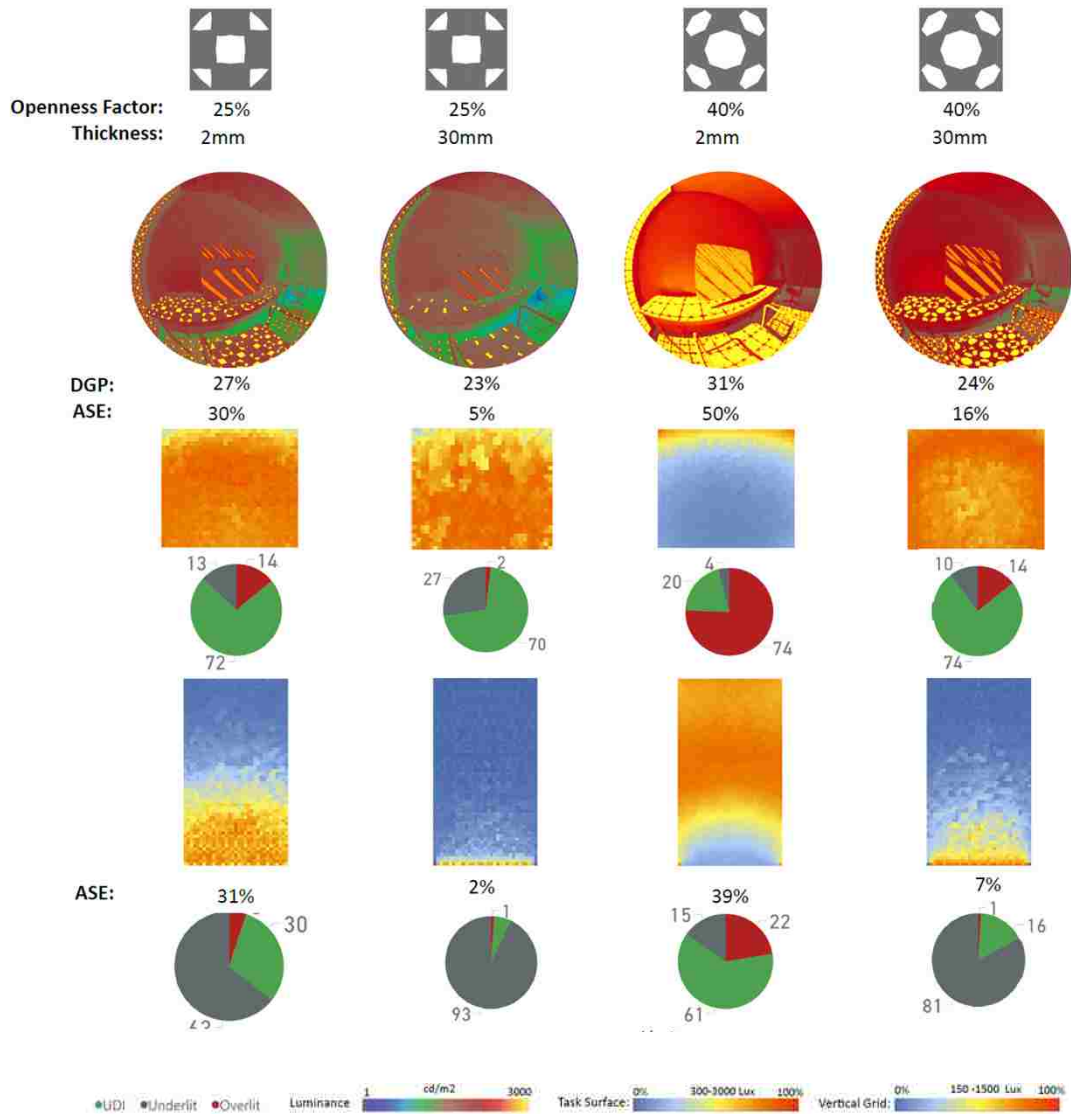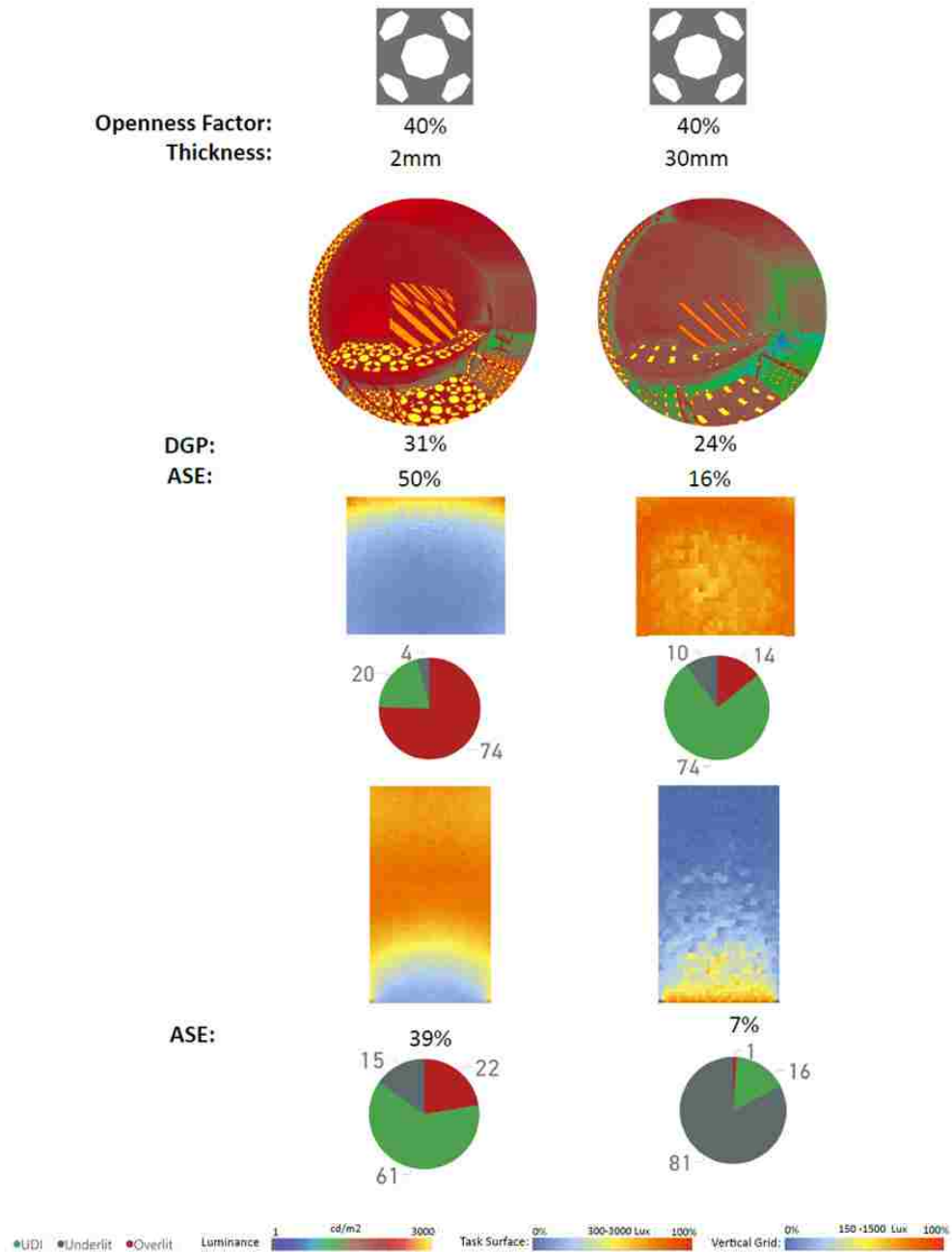
Figure 67: Wider openness factor diffuses light and darken the space

With a 40% openness factor, a drop in AES for both vertical and horizontal task surfaces provides the space with diffused lighting.

6.The presence of Sun:

Example: Museum, Lobby, Cafeteria, Hallways. The presence of sun is a special case scenario and is used in an environment where people would enjoy the theatrical nature of light. Any openness factor above 30% would provide the space with a lighting condition that is suitable for the playfulness of light.

Lower openness factor would generate dramatical light effects in the space, where as wider openness factors would increase the light presence in the room.

Thickness on the other hand would reduce glare, diffuse light which will decrease the playfulness of light in the space.
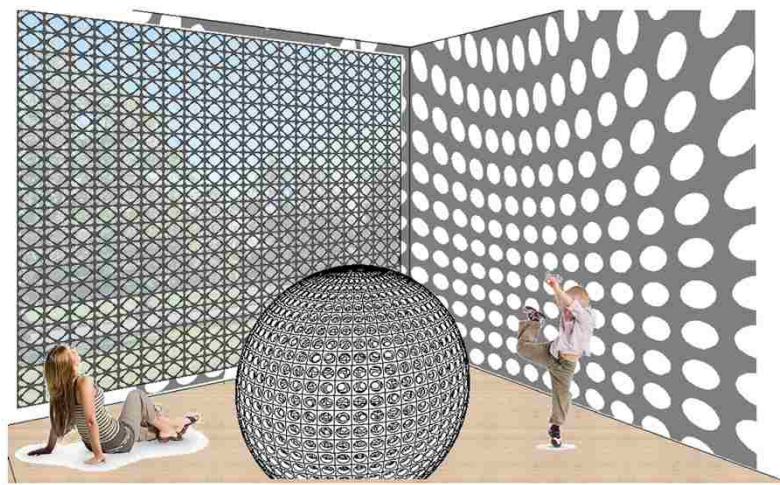

Presence of Sun:

DGP	>30%
ASE	>10%

Pattern Image																	
Openness Factor	5%	10%	15%	20%	25%	30%	35%	40%	45%	50%	55%	60%	65%	70%	75%	80%	85%
DGP	5%	24%	25%	28%	27%	29%	30%	31%	33%	35%	36%	38%	40%	40%	42%	44%	45%
UDI V	2%	41%	66%	74%	72%	64%	59%	50%	43%	38%	33%	29%	26%	23%	21%	20%	19%
Underlit V	96%	56%	30%	17%	13%	10%	9%	7%	7%	6%	6%	5%	5%	5%	5%	4%	4%
Overlit V	1%	2%	3%	7%	14%	24%	32%	41%	48%	55%	60%	64%	68%	71%	73%	74%	75%
ASE V	2%	4%	11%	20%	30%	39%	44%	50%	55%	59%	62%	64%	67%	68%	69%	70%	71%
UDI H	1%	6%	13%	23%	31%	38%	43%	49%	53%	56%	58%	60%	61%	61%	61%	61%	61%
Underlit H	96%	92%	84%	72%	62%	54%	47%	40%	34%	29%	25%	22%	19%	17%	16%	15%	14%
Overlit H	1%	2%	2%	4%	5%	7%	8%	10%	12%	14%	15%	17%	19%	20%	22%	23%	24%
ASE H	3%	14%	19%	25%	31%	35%	37%	39%	41%	43%	45%	47%	48%	49%	50%	51%	52%

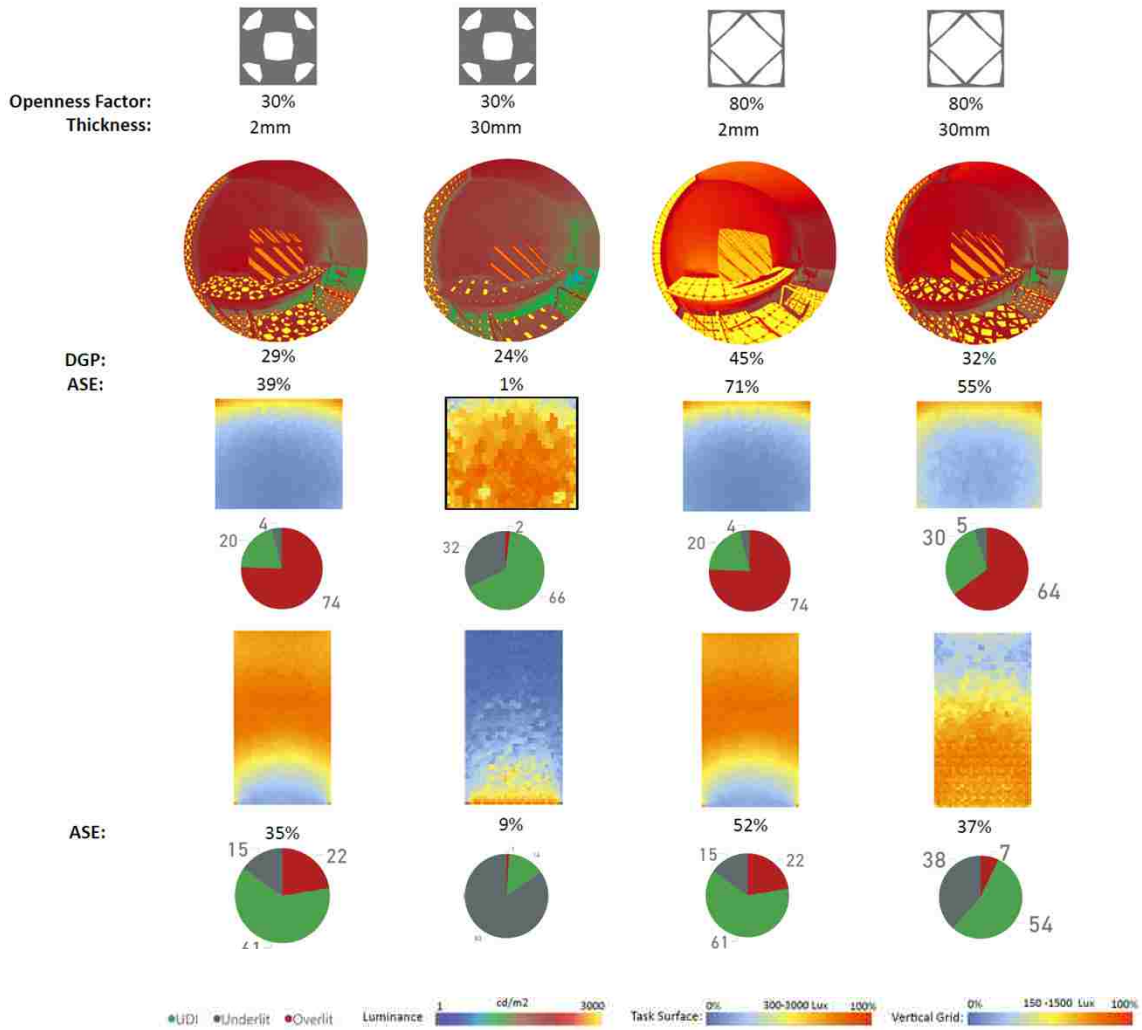**Table 11:** Suitable openness factors for the presence of sun

Figure 68: The effect of thickness on the playfulness of light .

CHAPTER 5
CONCLUSION

This thesis focuses on the effect of sun screen patterns on the daylighting performance of a given space. Initially, available methods for designing shading devices have been reviewed. These strategies include, solar geometry, insolation, thermal data and visual comfort.

Designing shading devices based on solar geometry is the most historical method. Cut-off dates and times are used to relate the position of the sun in the sky to the building element to be shaded and shading device is generated to provide shading in a given period. This method does not take weather data and surroundings into consideration. Two windows in two different cities with the same latitude have the same shading device regardless of their respective climatic conditions.

Designing shading devices based on insolation calculations processes weather files to calculate the direct and diffuse radiation. Direct and diffuse sunlight, cloud cover, wind, atmospheric turbidity, geometry and material of surroundings are taken into account to compute the amount of solar radiation falling on a given surface and shading devices are designed to prevent excessive radiation falling on windows and other building elements. However, this technique also is limited to the evaluation of insolation levels at the façade and does not incorporate the performance or the requirements of the space behind the facade.

Designing shading devices based on thermal loads is a relatively new technique. Although the prior two techniques can be used for generation of shading devices, this technique is based on testing different alternatives. The effectiveness of different shading devices are tested by calculating the annual heating and cooling loads; the alternative that provides the least amount of energy loads are selected.

Visual comfort is a another relatively new method used both for generating and testing shading devices. Although different daylighting metric could be used, the underlying premise is that human beings operate shading devices only when they are not visually comfortable. Based on the initial explorations of comparing different techniques (Chapter 2), daylighting and visual comfort is the chosen as the best method for designing screens. The explorations in this thesis are based on Islamic geometries, but the workflow is valid for any form and shape.

The main contribution of this thesis is to develop a workflow for generating and evaluating sun screens. This workflow demonstrates practices to overcome computational and simulation challenges that are inherently part of designing and evaluating screen patterns due to the geometric complexity and intensity. Generating these Islamic patterns require visual training and identifying the smallest module in a pattern that could be repeated. Simulating the patterns are time consuming. The smaller or thicker the openness factor, the longer simulation time. Therefore it is imperative to find the most efficient way of generating the patterns and running the simulations. Otherwise, the computational cost does become prohibitive.

The generated screens have complex geometries that presents interesting and phenomenal light effects on the interiors. Addressing the building performance and interior user comfort, two sets of patterns are selected for this thesis as a basis of comparison. Each pattern is generated with a 5% increments of openness factor starting from 5% till 95%. The daylighting evaluations are performed with horizontal and vertical UDI values, DGP results, and ASE quantities.

The results of point to the following findings:

•The design of the pattern does not affect the performance of the space on its own, and the openness factor determines the performance. That is, it is not necessary to repeat the evaluations for different patterns (of same thickness), because as long as the openness factor remain the same, two different patterns will yield the same performance outcome. The data obtained indicate that designers are free to generate a variety of floral or geometrical patterns with the same openness factor and get the same results.

•Thickness is another performance indicator. Although it may be impossible to achieve the desired outcome by simply changing the openness factor, combination of thickness and openness factor provide a methodology for achieving the intended daylighting performance.

•The selection of the openness factor and thickness varies depending on the functionality of the space. Spaces with predominantly horizontal tasks require a different screen designs than spaces with vertical tasks. Similarly, workspaces with highly controlled daylighting criteria requires different screen designs than spaces that require simple visual tasks. It is possible to use a single pattern and vary the openness factor and thick parameters over the façade to match with the functionality of the interior spaces.

5.1 FUTURE DEVELOPMENT:

In future the work can be expended to evaluate the cell count and size on the screen. Different materials will affect the screen geometry, as opaque materials will shade, and translucent materials will filter the light. An computational tool (plugin or a web based service0 could be provided to clients for making informed choices on shade screens. And last but not least, occupant studies would be useful to study the perceptual qualities of screens.

BIBLIOGRAPHY

Holl, S. (2011). Someone Has Built It Before on WordPress.com. Retrieved June 08, 2017, from https://archidialog.com/page/25/?blogsub=confirming

Hillenbrand, R. (2004). Islamic architecture: form, function and meaning. New York: Columbia University Press.

Movie interview with Sandeep Khosla on DPS Kindergarten School. (2016, November 16). Retrieved June 08, 2017, from https://www.dezeen.com/2013/11/04/movie-dps-kindergarten-school-by-khosla-associates/

DOE. Building Catalog: Case Studies of High Performance Buildings. https://buildingdata.energy.gov/home (Accessed on 12/6/2016).

Olgyay V and Olgyay A. Design with Climate: Bioclimatic Approach to Architectural Regionalism. Princeton NJ: Princeton University Press, 1963.

Schiller S. and Evans JM. "Teaching Architects Low Energy and Climate Conscious Design", Renewable Energy, 5(5), 1146-1150, 1994.

7 Group and Reed B. The Integrative Design Guide to Green Building. Hoboken NJ: John Wiley & Sons, 2009.

Mumovic D. and Santamouris M. A Handbook of Sustainable Building design and Engineering. London: Earthscan, 2009.

Stein B, Reynolds JS, Grondzik WT, Kwok AG. Mechanical and Electrical Equipment for Buildings. Hoboken NJ: John Wiley & Sons, 2006.

Roberts A, Marsh AJ, ECOTECT: Environmental Prediction in Architectural Education, Conference Proceedings, 19th ECAADE - Education for Computer Aided Architectural Design in Europe, Helsinki, Finland, 2001.

Arumi-Noe F. 1996. "Algorithm for Geometric Construction of an Optimum Shading Device." Automation in Construction, 5(3):211-217.

Etzion Y. 1992. "An Improved Solar Shading Design Tool". Building and Environment, 27(3): 297-303.

Kabre C. 1999. "WINSHADE: A Computer Design Tool for Solar Control." Building and Environment, 34(3):263-274.

Marsh A. 2003. "Computer Optimized Shading Design." International Building Performance Simulation Association (IBPSA) Conference, Eindhoven, Netherlands.

Marsh A. 2005. "Application of Shading Masks in Building Simulation." International Building Performance Simulation Association (IBPSA) Conference, Montreal, Canada.

Kaftan E. and A. Marsh. 2005. "Integrating the cellular method for shading design with a thermal simulation." Passive and Low Energy Cooling Conference (PALENC), Santorini, Greece, 965-970.

Olgyay A. and V. Olgyay. 1957. "Design with Climate: Solar Control and Shading Devices." New Jersey: Princeton University Press.
Shaviv E. 1975. "A method for the Design of External Sun Shade." Build International 8:121-150. Applied Science Publishers, UK.

Reinhart CF, Mardaljevic J and Rogers Z. "Dynamic daylight performance metrics for sustainable building design", Leukos, 3(1), July 2006, pp. 1-25.

Innoue T., T. Kawase, T. Ibamoto, S. Takakusa, Y. Matsuo. 1998. "The Development of an Optimal Control System for Window Shading Devices based on Investigations in Office Buildings." ASHRAE Transactions 104: 1034-1049.

Lindsay C.R.T. and P.J. Littlefair. 1992. "Occupant Use of Venetian Blinds in Offices." Building Research Establishment (BRE) Publications, PD233/92.

Littlefair P. 2002. "Control of Solar Shading." Building Research Establishment (BRE) Information paper.

Inkarojrit V. 2008. "Monitoring and Modelling of Manually-Controlled Venetian Blinds in Private Offices: A Pilot Study." Journal of Building Performance Simulation 1(2): 75-89.

Van den Wymelenberg K. 2012. "Patterns of Occupant Interaction with Window Blinds: A literature Review." Energy and Buildings 51(2012): 165-176.

Pérez-Lombard, L.; Ortiz, J.; Pout, C. A review on buildings energy consumption information. Energy Build. 2008, 40, 394–398.
Boubekri, M.; Hull, R.B.; Boyer, L.L. Impact of window size and sunlight penetration on office workers' mood and satisfaction a novel way of assessing sunlight. Environ. Behav. 1991, 23, 474–493.

ASHRAE. (2004). ASHRAE Standard 55-2004 Thermal environmental conditions for human occupancy. Atlanta, GA: American Society of Heating, Refrigerating, and Air-Conditioning Engineers.

Huizenga, C., Zhang, H., Mattelaer, P., Yu, T., Arens, E., and Lyons, P. (2006). Window performance for human thermal comfort. Center for the Built Environment, Berkeley, CA: University of California.

Human Thermal Comfort | Sustainability Workshop
https://sustainabilityworkshop.autodesk.com/buildings/human-thermal-comfort

A. (2013). Sustainable facades. Design methods for high-performance building envelopes. Bognor Regis: John Wiley & Sons Ltd.

Larson, G. W., & Shakespeare, R. (2003). Rendering with radiance: the art and science of lighting visualization. Davis: Space & Light.

Khoo, Chin Koi, Salim, Flora, D., Mattern, Friedemann, Santini, Silvia, Canny, John, F., Langheinrich, Marc, & Rekimoto, Jun. (2013). Lumina: A soft kinetic material for morphing architectural skins and organic user interfaces. Pervasive and Ubiquitous Computing Proceedings
of the 2013 ACM International Joint Conference, 53-62.

Reinhart C F, Galasiu A. 2006. Results of an Online Survey of the Role of Daylighting in Sustainable Design. NRC-IRC Report.

Roe, S. (2013). Information storm. Open Systems - Proceedings of the 18th International Conference on Computer-Aided Architectural Design Research in Asia, CAADRIA 2013, 915-924.

Robinson, D., & Stone, A. (2005). Irradiation modelling made simple: the cumulative sky approach and its applications Plea2004 - The 21st Conference on Passive and Low Energy Architecture. Eindhoven, The Netherlands, 19 - 22 September 2004

Aksamija, A. (2014). High Performance building envelopes: Design methods for energy sufficient facades.

DiLaura, D. L. (2011). The lighting handbook: reference & application. New York, NY: Illuminating Engineering Society of North America.

Figure 7: "History of Precolonial North America." History of North America | Essential Humanities. N.p., n.d. Web. 28 Feb. 2017.

Figure 8: Co., Mint Design. "Native American Heritage of Santa Fe." Coastal Breeze News. N.p., n.d. Web. 28 Feb. 2017.

Figure 9: https://s-media-cache-ak0.pinimg.com/736x/0b/c6/2e/0bc62ee8ce3030e1f6ebab08344ddb38.jpg

Figure 11: "Gibraltar Airport by Bblur Architecture and 3DReid." Dezeen. N.p., 08 Mar. 2013. Web. 28 Feb. 2017.
Horsley, Carter B., Emily Nonko, Dana Schulz, Metro New York, Michelle Cohen, Diane Pham, Jon Dioffa, and Annie Doge. "Not Tall Enough! On the World's Stage, New York's Supertalls Are Ungraceful Runts." 6sqft. N.p., 16 May 2016. Web. 28 Feb. 2017.
"Japan Photo Archive | Asakusa Culture Tourist Information Center - Kuma Kengo." Japan Photo Archiv | Asakusa Culture Tourist Information Center - Kuma Kengo. N.p., n.d. Web. 28 Feb. 2017.

Figure 18: "Light Matters: Mashrabiyas - Translating Tradition into Dynamic Facades." ArchDaily. N.p., 28 May 2014. Web. 28 Feb. 2017.

Fgure 20: Reinhart, c (2001). Daylight availability and manual lighting control in office buildings- simulation studies and analysis measurement.
Figure 21: "Sky Subdivision." Sky Subdivision | Natural Frequency. N.p., n.d. Web. 28 Feb. 2017.

Figure 27: Original: Mecjey C, Sadeghipour, M (2015) Woods Bagoot workshop (NY), Edited by Author
Figure 30: Larson, G. W., & Shakespeare, r. (2003). Rendering with radiance: the art and science of lighting visualization. Davis: space & light.
Figure 34-35: Mossati, Corinne. "Institut du monde arabe, paris." Gourmantic, 11 Jan. 2011. Web. 28 Feb. 2017.
Figure 36-37: "Metal that breathes: bloom installation made with 14000 thermobimetal pieces - evolo | architecture magazine." evolo architecture magazine rss. Evolo, 26 oct. 2012. Web. 28 feb. 2017.
Figure 40: Angawi A. Workshop, Jeddah.
Figure 42- 43: History of Islamic Architecture, Lecture, 2017, Effat University.